NOVEL SMALL-MOLECULE INHIBITORS OF MYCOBACTERIAL RNA POLYMERASE “AAPS”

By

SOMA MANDAL

A Dissertation submitted to the

Graduate School-New Brunswick

Rutgers, The State University of New Jersey

in partial fulfillment of the requirements

for the degree of

Doctor of Philosophy

Graduate Program in Chemistry and Chemical Biology

Written under the direction of

Prof. Richard H. Ebright

and approved by

_____

_____

_____

_____

New Brunswick, New Jersey

January 2014

ABSTRACT OF THE DISSERTATION

NOVEL SMALL-MOLECULE INHIBITORS OF MYCOBACTERIAL RNAP "AAPS"

By: Soma Mandal

Dissertation Director:
Dr. Richard H. Ebright

Tuberculosis global epidemics is a serious threat to human population, the disease is estimated to be the second highest cause of death due to infection. In this study we present a lead hit-compound "AAP1" identified through high-throughput screening performed against *Mycobacterium tuberculosis* RNA polymerase (RNAP). AAP1 displays great potential as a mycobacterial RNAP inhibitor and mycobacterial growth inhibitor.

AAP1 can be synthesized from commercially available precursors in single reaction step. AAP1 has a modular structure, facilitating the synthesis of novel AAP1 analogs and facilitating the interpretation of structure-activity relationships for novel AAP1 analogs. Currently, more than 400 AAP1 analogs have been synthesized and tested and based on improved characteristics, an AAP1 analog AAP12 is used in this study with AAP1 (AAPs).

By isolating, sequencing, and characterizing spontaneous resistant mutants, we have shown that mycobacterial RNAP is the functional cellular target for the antibacterial activity of AAPs

By isolating, sequencing, and characterizing resistant mutants, we have shown AAPs function through a site on RNAP that is different from, and does not overlap with the binding sites for rifamycins. The site is located at the base of RNAP "□ lobe" and N'-terminal of β' bridge helix and corresponds, essentially exactly, to the site for CBR703, a compound that does not inhibit mycobacterial RNAP and does not inhibit mycobacterial growth. It appears that AAPs are mycobacterial-specific ligands of RNAP β lobe and that CBR703 is a Gram-negative-specific ligand of the RNAP β lobe.

By observing the effect of AAPs on individual transcription step, we have shown that AAPs affect the nucleotide addition cycle of RNAP. Based on the fact that AAPs interfere with the nucleotide addition cycle of the RNAP without making any contact with the active center residues we propose that AAPs function allosterically by binding at the N-terminal sub-region of β' bridge helix, and by interfering with its conformational dynamics

In our current work, we are systematically preparing and evaluating novel AAP1 analogs. The objectives are to increase the antimycobacterial potency, to improve physical and pharmacological properties, and to identify compounds suitable for evaluation in an animal model of tuberculosis.

Acknowledgement

First and foremost I would like to express my gratitude towards my advisor Dr. Richard H. Ebright, this work is possible because of his help, support and faith. I would have never been able to surpass the hurdles without his guidance and help. I will be indebted to him for giving me the opportunity and encouragement, when I most needed it. His enthusiasm and passion towards science is inspirational and highly motivating and I consider this opportunity to learn from him as an enriching experience. My deepest and heartiest regards to him always.

I would like to thank Dr. Yon W. Ebright for all the help and guidance, and always being kind to me. From providing me suggestions about science, to providing me food, teach me about automobiles she has always been a friendly support. Thanks Yon !

I would like to thank my committee members Dr. Edward Arnold, Dr. Wilma Olson and Dr. Bryce Nickels for their suggestions and direction.

I would like to thank all the present and past members of our lab, and especial mention Dr. David Degen, Dr. Yu Zhang, Dr. Yu Feng, Carol, Dr. Ashish Srivastava, Dr. Sukhendu Mandal and Dr. Yi Jiang for always eagerly helping me and patiently answering my endless questions.

Next I would like to thank, my family away from home, my friends. They have been a constant support and help. I would like to thank Bodhana Dhole, Yashodhara Dasgupta, Crystal Maung, Princy Varughese, Priti Tiwari, Ramya Rao, Prasad Subramaniam, Nisha Mittal, Rochak Vig, Sugandha Sharma and Deepankar das. Thanks for making my journey of graduate school cherishable and memorable. Each of them has made immense contribution in this journey. From being bullied by me, to providing me with

food, listening to my endless complaints, or accompanying to emergency room and still enduring me and standing by me as “FRIENDs”. I know I cannot summarize all of your kind gestures and my feelings in words, thank you all for your love and kindness.

Last but certainly not the least I would like to thank my family. My father; he is an inspiration and my role model. My father and mother; has dedicated their life in bringing up me and my brother and making sure our life was always happiest and comfortable. My father has always been my guide in discerning between right and wrong. My mother has always stood as a pillar of strength and kindness. My brother; he has being my true strength and inspiration. Borda; he has always been a sense of hard work and endurance. They have always successfully made sure; I am safe, healthy and happy each and every day. This would have been impossible without all your love, support and guidance. I consider myself blessed to have you all as my family. I do not know how to express my gratitude towards these special people in words and the reasons are endless. Also, like to thank my chorda and extended family. My Jethu, Jemmuni who always made me feel special and joyous. My grandparents for their love and believe.

Dedication

To my Baapi, Ma and Podinana

Dedication

In memory of my Jethu, jemmuni and Grand parents

List of tables:

.

.

List of Figures

Table of contents

1. Introduction

1.1 Multi-subunit RNA polymerases (RNAP)

Transcription is the process by which RNA is synthesized from DNA template; this is the first and the most regulated step of gene expression. In archea, bacteria and eukaryotes transcription is performed by enzymes called as “multi-subunit RNA polymerase” (RNAP). Bacteria and archea contain only one RNAP, whereas eukaryote contains three multi-subunit RNAP known as, RNAP I, RNAP II and RNAP III. RNAP is conserved both structurally and functionally in all the three domains of life [1, 2]. All multi-subunit RNAP consists of at least five subunits, in bacteria they are β’, β, αI, αII and ω and in archea they are known as A, B, D, L, K [2, 3]. In eukaryotic RNAP II the subunits are termed as RPB1, RPB2, RPB3, RPB11, and RPB6. Archea and eukaryotes contains additional subunits [2, 4].

Bacterial multi-subunit RNAP is the simplest form of multi-subunit RNAP and is considered as a good candidate for structural and functional study [3]. Also, bacteria contain only one type of RNAP, essential for survival, hence bacterial RNAP is considered as a good antibiotic target [5, 6]. High resolution crystal structure is available for bacterial RNAP from various species such as *Thermus thermophilus*, *Thermus aquaticus* and recently from *Escherichia*. *coli* [7-11]. These crystal-structures provide substantial knowledge about the structure and function of RNAP. Also, many crystal structure of bacterial as well as eukaryotic RNAP bound with RNAP-inhibitor is available, these structures provide great deal of information about the structural and mechanistic basis of inhibition [12-15]. The information acquired from the structural details of

inhibitor binding can provide significant information for prediction of structure-activity relationship (SAR) hence help in optimization of inhibitor structure to improve potency. Additionally, structure of RNAP-inhibitor also, shed light on the functional mechanism of RNAP. various functional intermediate of the enzyme, which is otherwise hard to trap and elucidate.

1.1.1 Bacterial RNA polymerase core

n bacteria multi-subunit RNAP core is of almost ~400 kDa and consists of five subunits β', β, α_I, α_{II}, and ω. RNAP core has shape reminiscent to a crab claw and its dimension is observed to be ~150Å, ~100 Å, ~100 Å [2, 7]. In bacterial RNAP, β' and β are the two largest subunits and they form each pincer of the crab claw shape. The β and β' subunits also forms structural determinants responsible for interaction with DNA, RNA, DNA:RNA hybrid, substrate uptake and catalysis (Figure 1) [2-4]. The two α subunits initiates the assembly of RNAP and forms the base that tethers the two largest subunits [7, 16, 17]. RNAP core is catalytically competent, but is inadequate to begin transcription with DNA sequence specificity and processivity. It requires another protein factor or initiation factor called "σ" to perform transcription initiation with DNA sequence specificity and processively [18].

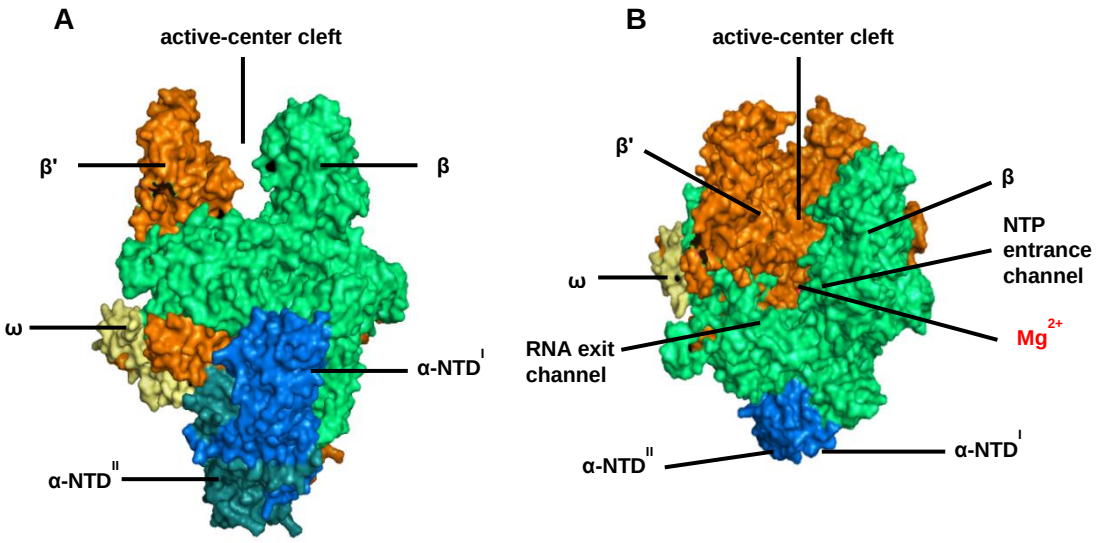

Figure 1: Structure of bacterial RNAP core

Structure of T. aquaticus RNAP core at 3.3 Å. β' subunit is in orange β in green, α-NTD^{I} and α-NTD^{II} in blue and ω in light yellow. Atomic co-ordinates obtained from PDB accession code 1HQM

A) Upstream view B) Top view

1.1.2 Bacterial RNAP core subunits

In bacterial RNAP β' is the largest subunit and the MW is ~ 160 kDa. The gene that encodes the β' subunit is called *rpoC*. It forms one of the pincer in the crab claw shape; and is comprised of a central mass connected with two smaller lobes [2]. The β' subunit

makes interaction with DNA, RNA and DNA:RNA hybrid [19, 20]. It forms part of the active center or catalytic center (Nucleotide addition reaction takes place), and contains the highly conserved sequence " NADFDGD" located near the active center containing the three aspartate residues that co-ordinates the $Mg^{2+}{}_{I}$ ion essential for catalysis [21]. The β' subunit also forms two functionally important structures, located close to the active center called trigger loop and bridge helix. Both, the trigger loop and the bridge helix plays important role in catalysis [22].

The β subunit in bacterial RNAP is ~ 155 kDa and is the second largest subunit. The gene that encodes β subunit is called *rpoB*. It forms the other pincer in the crab claw structural model; it also composed of a central mass connected with four smaller lobes [2]. The β lobe is a mobile domain which can undergo movement respect to the remaining subunit [23]. The β subunit makes interaction with DNA, RNA and DNA:RNA hybrid and together with the β' subunit forms the catalytic center [3].

The β and β' subunits makes extensive contact with each other and together forms important functional determinants

The active center cleft, as the name suggests is a spit, it traverses between the β' and β pincer, and ends at the base of the active center (where Mg^{2+} ion is present) [7]. This cleft has a diameter of ~ 25 Å, which is sufficiently large enough to accommodate duplex DNA.[2, 7]. The duplex DNA utilizes this channel to load onto the RNAP to reach the active center [24].

The RNA exit channel, it is a tunnel with dimension 25 Å X by 20 Å, it begins at the base of the active center cleft and ends at the surface of RNAP on one side of the active center cleft, during transcription elongation the nascent RNA exit through this tunnel [7, 19, 20, 24].

The NTP entrance channel or secondary channel, through this tunnel NTP diffuses to reach the active center. It has a dimension of 20 Å by 10 Å.[7, 19] This tunnel connects from the base of the active center to the surface of RNAP [24]. Additionally many protein factors also utilize this channel to reach the active center [25].

The catalytic center or active center is located at the base of the active center cleft and is marked by the presence of the Mg^{2+}, ion. It contains the site for binding of the RNA 3'- termini called as "i site" [26]. It also contains the site for binding of the incoming NTP "i+1" site [27, 28].

The switch region is located at the base of the β' pincer and is consists of five switches. They are called as switch 1 through 5, switches 1, 2, 5 is made by the β' subunit residues and 3, 4 by the β subunit residues.[14] The switch region controls the opening and closing of the β' clamp and hence, controls the loading of DNA [29].

The hybrid Binding site is also formed the two largest subunits of the RNAP is present between the active center and the bridge helix [30]. It holds and maintains the 8-9 bp DNA:RNA hybrid during RNAP initiation and elongation [19].

α subunit is the third largest subunit in RNAP and is present in two copies α^{I} and α^{II} [16]. The gene that encodes α subunit is called *rpoA.* Both the subunits have identical sequences but they differ in the way they interact with RNAP core and hence, differs structurally [16]. Each α subunit can be divided into N-terminal (α-NTD) and C-terminal (α-CTD) domain connected via a flexible linker [7, 31, 32]. α^{I}-NTD makes interaction with the β' subunit and α^{II}-NTD makes interaction with the β subunit [16]. Together α^{I} and α^{II} forms the base of the RNAP and tethers the β' and β subunits together [7, 16, 32]. α initiates the assembly of RNAP by forming α-NTD dimer which interacts with the β subunit followed by β'ω. The assembly pathway can be depicted as:

$\alpha \rightarrow \alpha_2 \rightarrow \alpha_2\beta \rightarrow \alpha_2\beta\beta\omega$ [17]. α-CTD plays important role in transcription regulation (by interacting with transcription regulator like catabolite activator protein etc.) and promoter recognition (some promoter) [33].

ω is the smallest subunit in RNAP and it interaction mainly with β'. The gene that encodes ω subunit is called *rpoZ*. The ω subunit of RNAP is not essential for its function; enzyme lacking ω can undertake catalysis [34]. It functions as a molecular chaperone and assists in the folding of the β' subunit. It is believed to act as a latch, in which it holds the N-terminal and C-terminal end of the largest subunit of RNAP and helps it fold by reducing it configurational entropy [35]. In the available crystal structures of RNAP it is observed to make contact with the β' subunit and is present on the outer surface of RNAP farther from active center [3, 7, 32].

1.2 RNA polymerase holoenzyme:

RNAP core binds to a dissociable initiation factor called σ to form "RNAP holoenzyme" (Figure 2) [36]. This form of the enzyme is competent to perform, DNA sequence specific and prossesive transcription. σ plays important role in recognizing specific DNA sequence "promoter sequence" and in melting (unwinding) the duplex DNA in the region -11 to +2 (+1 designated as the start site) [37]. Most bacteria contain several σ factors, and the association of specific σ factor with RNAP core depends on the growth conditions and specific transcriptional requirement of the cell [38]. Most bacteria contain one σ factor for the synthesis of house-keeping genes called as primary σ or house-keeping factor. In *E. coli* the primary σ is known as σ^{70} (molecular weight ~70 kDa) and for other bacteria the same is known as σ^{A}. In *E. coli* The gene that encodes σ^{70} is

called as *rpoD* and for other bacteria σ^A gene is called as *sigA* [39, 40]. Crystal structures are available for RNAP holoenzyme and they provide structural details of interaction between σ^A and RNAP core [32, 41, 42]. Also recently some high resolution structure is determined which presents detailed information of σ^A, interaction with promoter DNA [32, 43].

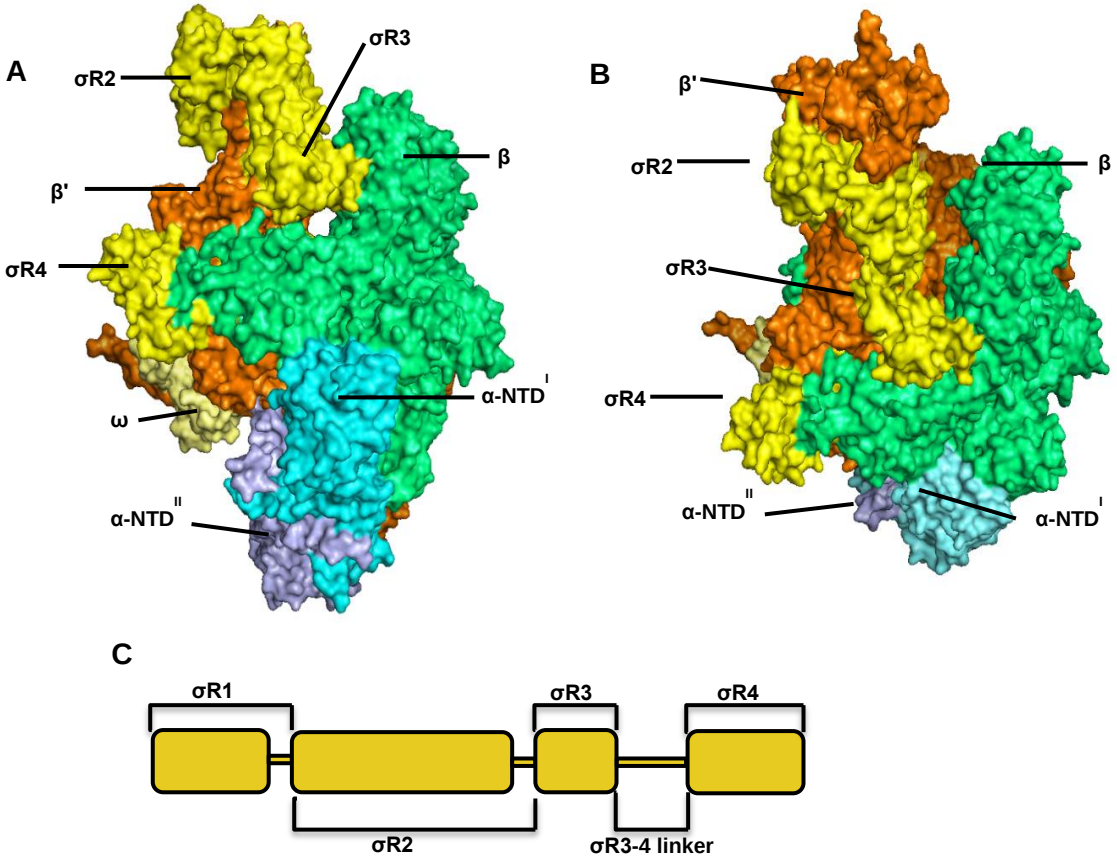

Figure 2: Structure of RNAP holoenzyme and σ^A domain organization

RNAP holoenzyme T. thermophilus at 2.6 Å. β' subunit in orange color, β subunit in green color, α-NTDI and α-NTDII in blue and cyan and blue respecivetly,ω in light yellow and σ^A in yellow. The atomic co-ordinates are taken from PDB accession code 1IW7.

A) Upstream view B) Top view C) σ^A domain organization

σ makes extensive interaction with RNAP β' and β subunit, it contains 4 conserved regions namely σ Region1 (σR1) or σ Region1.1 , σ Region2 (σR2) or σ Region1.2-2.4, σ Region3 (σR3) or σ Region3.1, and σ Region4 (σR4) and a flexible region called σ Region3-4 linker or σ Region 3.2 (Figure 2) [43]. σR1 is located at the N-terminal, it is non-globular or unstructured and is highly negatively charged. It has determinants which autoregulates binding of free σ with promoter DNA (which is when not bound with RNAP core), σR1 interacts with σR2 and σR3 and prohibits it from interacting with DNA [44, 45]. σR1 also plays important role in interaction of σ with RNAP core; it acts as a DNA mimic and interacts with the active center cleft [46].

σR2 is globular, it primarily interacts with β' subunit and domain in promoter recognition. It is interacts with promoter -10 region and unwinds double stranded DNA in this region [32, 47]. Recently structural details is available for RNAP initiation complex; it demonstrates structural basis of interaction between σR2, promoter -10 elements and discriminator element [48]. σR3 is a structured globular domain, it contains determinant for interaction with RNAP core; it participates in interaction with DNA (promoter -10 extended elements) [32]. σR3-4 linker is unstructured, it is highly negatively charged and acts as a RNA mimic, it occupies the RNA exit channel in the absence of elongating RNA [43]. σR4 is the C-terminal domain of σ; it is structured and interacts with the tip of the β flap. It interacts with promoter DNA -35 elements and also binds to transcriptional regulator [36, 43, 49].

1.3 Promoter DNA:

Promoter sequences are specific DNA sequence, which are recognized by RNAP holoenzyme to initiate transcription. Bacterial promoter sequences are marked by the presence of two specific region “-10” and “-35”, they are located upstream of the start site which is “+1” [50]. The consensus sequence at -10 region in bacterial promoter is 5’-TATAAT-3’ and it is recognized by σR2 [37, 50]. The consensus sequence at -35 region in bacterial promoter is 5’-TTGACA-3’, -35 region is recognized by σR4 [43, 50]. The -35 and -10 regions are generally separated by 17 bp DNA, this 17 bp spacer DNA is non-conserved [51]. Some bacterial promoter contains additional determinants for interaction with RNAP holoenzyme. The discriminator element is located immediately upstream of -10 element with the consensus sequence 5’-GGGA-3’, this DNA sequence makes specific interaction with σR2.[48, 52, 53] The -10 and -35 DNA sequence are referred to as core promoter sequence. Some promoters may contain additional upstream -10 and -35 region of recognition [54]. The strength (interaction with RNAP holoenzyme) of the promoter is determined by the core element sequence and presence of other recognition site.

1.4 Transcription

Transcription is the process by which RNA polymerase transcribes the information stored in DNA into RNA. In bacteria this the most regulated step, and is followed by

translation of the RNA sequence into amino acid. Transcription is a multi-step process and can be broadly divided into three main steps initiation, elongation and termination.

1.4.1 Initiation

RNAP holoenzyme interacts with promoter DNA; binds to it and forms RNAP close complex (RP_c), in RP_c the DNA remains outside the active center cleft. This is an unstable complex, it can easily dissociates or isomerize into a stable state in which the DNA enters the RNAP active center cleft but remains double stranded, this state is called as the RNA polymerase intermediate complex (RP_i) [55, 56]. Followed by formation RP_i, the enzyme unwinds up to 13 nt of DNA (-11 to +2) this is RNAP open complex or RP_O. In RP_O the DNA displaces σR1 from active center cleft and the DNA is secured by closing of the β' clamp (β' clamp rotates ~11° with respect to RNAP holoenzyme) [29, 46, 55]. In the next step of transcription initiation the enzyme syntheses 2 to 10 nt of RNA, while still retaining contact with promoter and scrunching or pulling the downstream DNA into the active center, in this state the "enzyme complex" is called as RNA polymerase initial transcribing complex or "RP_{itc}"[57-59].

$$\mathbf{R+P \rightarrow RP_c \rightarrow RP_i \rightarrow RP_o \rightarrow RP_{itc}}$$

During RP_{itc} the polymerase goes through various cycles of synthesis of short RNA (2-10 nt) called as "abortive initiation" [60, 61].

1.4.2 Elongation

RNA polymerase enters elongation complex ("RNAP-EC" or RD_e) when it syntheses >10 nucleotide of RNA and escapes from the promoter DNA. In this state the RNAP enter processive synthesis of RNA and it is a very stable complex. During transcription elongation the DNA remains in the active center cleft, the transcription bubble is maintained at 12 nt and the clamp remains closed [29, 62]. During RD_e a constant length of 9-10 bp of DNA:RNA hybrid is maintained, this hybrid binds very tightly to RNAP and confers stability to the elongation complex [63]. The RNA product in this stage is sufficiently large enough (>1) to enter the RNA exit channel and it displaces σ R3/4 linker [41]. Also, during the RP_e the σ subunit can optionally release from the RNAP core [38, 64].

$$\mathbf{R+P \leftrightarrow RP_c \rightarrow RP_i \rightarrow RP_o \rightarrow RP_{itc} \rightarrow RD_e}$$

During elongation the enzyme undergoes, repeated cycles of nucleotide addition to the hydroxyl group of nascent RNA 3' terminus, and translocation [22]. The nucleotide addition cycle (NAC) is elucidated by various biochemical studies and crystal structures evidence from pol II and bacterial RNAP [26-28, 65-67]. The nucleotide addition cycle can be divided into three steps:

1. Entry of NTP through the secondary channel, and binding of the correct NTP (complimentary to non-template NTP at i+1 site) at the pre-insertion site, the trigger loop then adopts a closed conformation (which is folds into alpha-helical conformation), delivering the NTP to the insertion site (required for catalysis) [27, 68]. The trigger loop ensures the selection of correct NTP and hence, guarantees transcription fidelity [66].

Binding of the nucleotide at the correct position requires assistance of another structural module located near the catalytic center; the β' subunit bridge helix [27].

2. The second step is catalysis; which is transfer of the nucleotidyl moiety from the incoming NTP to the 3' terminal hydroxyl group of the growing RNA by formation of a phosphodiester bond and release of a pyrophosphate molecule. This reaction follows a SN_2 (substitution nucleophilic bimolecular) mechanism and requires the presence of two Mg^{2+} ion [69]. The first Mg^{2+} ı ion is present at the catalytic site, chelated by three aspartate residues of the β' subunit [21]. This Mg^{2+} ion activates the 3' hydroxyl group of the RNA 3' terminus, an also binds with the incoming NTP α-phosphate group [58]. The second Mg^{2+} ion is weakly bound and is brought in by the incoming NTP [70]. This Mg^{2+} ion shields the negative charge of the incoming NTP by coordinating with β and γ phosphate and also helps stabilizes the pent covalent transition state. Crystal structure evidence suggests during addition of the NTP the trigger loop remains in a closed or folded state, which facilitates the phosphodiester bond formation [66]. Followed by the release of the pyrophosphate ion the trigger loop adopts an open or un-folded conformation. Thus during the NTP addition the trigger loop cycles between the open unfolded state and the closed folded state facilitating NTP addition and phosphodiester bonds formation [71].

3. Followed by the phosphodiester bond formation between the incoming NTP and the 3' hydroxyl group of the growing RNA, the insertion site in the RNA polymerase active center remains occupied by the newly formed RNA-3' (this state is the pre-translocated state). Translocation involves moving of the newly formed RNA-3' end by one register to make the insertion site available for the new NTP, this state is called as "post-translocated" state [22]. Crystallographic and biochemical evidence suggests that in RD_e the transition from pre-translocated state to post-transloacted state involves bending

of the bridge-helix and rearrangement of the trigger loop.(Crystal structure is available in which the trigger loop and the bridge helix are observed to adopt multiple structural conformation state) [32, 72-74]. Based on these crystallographic observation it is proposed that during translocation the bridge helix undertakes a bent conformation (present as a straight helix), and the trigger loop in a wedged conformation contacting the bridge helix [75]. This conformational dynamics of trigger loop and bridge helix assists the newly formed DNA:RNA hybrid to move out of the active center and to allow the next template (DNA) base to enter the pre-templating position [76]. Following this transition of the template base, the bridge helix relaxes, which allows the next template base to occupy the active center by flipping out 90°[22]. Single molecule experiment observation suggests that RNAP in elongation complex uses a stepping mechanism in which it moves 1 nt per addition cycle and also supports the Brownian ratchet model.[77] In the RNAP ratchet model it is proposed that in RD_e the enzyme is in equilibrium between the pre-translocated state and the post-transloacted state, and binding of NTP stabilizes the post-translocated state [73]. Also, the pyrophosphate release after catalysis, (which remains between the bridge helix and closed trigger loop) re-mobilizes the trigger loop, which contacts the bridge helix and bends it; assisting in translocation [78].

During elongation the enzyme can experience interruption like incorporation of a wrong nucleotide, pause or arrest. RNAP utilizes various mechanisms to overcome these temporary states. When a wrong NTP is incorporated the enzyme uses various proofreading mechanism to correct it, the main proof-reading mechanisms are pyrophosphorolytic editing and hydrolytic editing of the misincorporated NTP. In bacterial cell the enzyme primarily undergoes factor (Gre) dependent hydrolytic proofreading [79, 80].

During transcription elongation the enzyme sometime experience temporary stalling called as “pause.” Pause can be caused DNA sequence dependent, due to incorporation of wrong NTP, DNA lesion or due to formation of secondary structure by nascent RNA. Pause can also be caused by RNA backtracking, where RNAP moves backward on the DNA template [22]. Pause caused by these factors is called as elemental pausing and is an off-track state [81]. The enzyme also experience factor dependent pausing (like σ.), all pauses are temporary state and RNAP uses various mechanisms to resolve this state [82]. When Interruption in elongation can also occurs due to DNA damage or due to specific sequence and the enzyme stalls for a longer time and can be rescued by external protein factor for resume its movement, such a state is “arrest” [83, 84].

1.4.3 Termination

Termination is the last step in transcription; in this step the RNAP stops synthesizing RNA and dissociates from the DNA and RNA. After termination the same RNAP molecule can start transcription from some other promoter DNA. Termination can be factor-independent which is caused by secondary structure formation by the nucleic acid molecule or factor dependent.

1.5 Bacterial RNA polymerase as an antibacterial drug target:

Bacterial RNAP is considered as an attractive drug target for three primary reasons:

1) RNAP is an essential enzyme for survival of organism and bacteria contains only one type of RNAP (no alternate mechanism for survival). Hence, targeting bacterial RNAP confers bactericidal property to the inhibitor enhancing efficacy.

2) Bacterial and eukaryotic RNAP is structurally and functionally conserved, but they do not share extensive sequence similarity [2]. This confers the inhibitor with therapeutic selectivity, required for an antibiotic drug (makes the inhibitor specific for targeting bacterial RNAP without affecting the eukaryotic cells).

3) RNAP is highly conserved structurally and sequentially amongst bacteria this makes it a drug target candidate that can provide a broad spectrum antibiotic [3].

All the above properties collectively make RNAP a promising drug target; an excellent example of bacterial RNAP inhibitor drug is rifamycin class of inhibitors and various other known RNAP inhibitor antibiotic. (myxopyronin, lipiarmycin, CBR703 etc.). (Lipiarmycin is also an approved drug for treatment of bacterial infection.)

RNAP-inhibitor complexes act as chemical probes for determination of structure and mechanism of the enzyme. Study of the structure and mechanism of RNAP with the inhibitor myxopyronin sheds light on the importance of the mobile switch region of the enzyme and also elucidates the importance of clamp movement in RNAP activity [14, 29] In the past crystal structure of the RNAP-inhibitor complex was able to capture transient and otherwise hard to detected intermediate state; an example is crystal

structure of yeast RNAP bound with α-amanitin presenting a translocation intermediate which was never observed previously [85-87].

1.6 Antibiotics with bacterial RNA polymerase as target

1.6.1 Rifamycin

The rifamycin antibacterial agents were first isolated in 1957 and are the first class of antibacterial agents and drug known to inhibit bacterial RNAP [88]. Rifamycins belong to the ansamycin family of compounds produced naturally by bacteria *A*. *mediterrane*i. [89]. They are macro cyclic compound composed of naphthyl moiety and ansa rings (Figure 3) [90]. There are many semi-synthetic varieties of rifamycins, the most important are 1) Rifampicin or Rifampin 2) Rifabutin and 3) Rifapentine [15, 89, 90]. They are extremely potent broad spectrum antibiotics and are used clinically as drug against bacterial infection [91]. Rifampicin is considered very important for their role in TB treatment as it is one of the primary line antibiotic used to treat the disease, and also one of the few drugs known to target and disinfect the bacilli in latent TB [92].

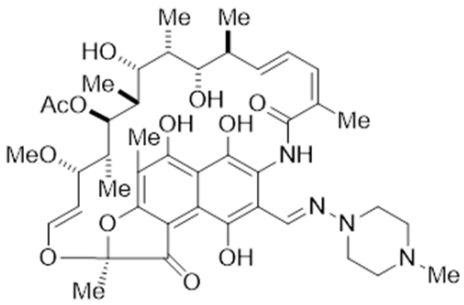

Figure 3: Structure of rifampicin

The functional cellular target of rifamycins is determined to be the bacterial RNAP. Previous studies indicate that mutations that confers rifamycin resistance in bacteria (*E. coli*, *M. tuberculosis* etc) maps within the RNAP β subunit and entirely with in the *rpoB* gene [93, 94]. The structural basis of rifamycin binding to RNAP is determined through X-ray crystallography at 3.2 Å resolution (Figure 4) [12]. The rifamycin binding pocket lies adjacent to the active center, but does not overlap with RNAP catalytic center. Rifamycin binding determinants lies entirely within RNAP β subunit region of bacterial RNAP (Figure 4) [12, 15].

Biochemical and structural evidence sheds light on the mechanism of transcription inhibition by rifampicin [12]. It inhibits the formation of RNA product >2-3 nt, it does not affect transcription abortive initiation (up to 2-3 nt RNA product) or elongation [12, 95]. Hence it is believed that rifampicin inhibits RNAP through simple steric blockage of the elongating RNA product at 2-3 nt [12].

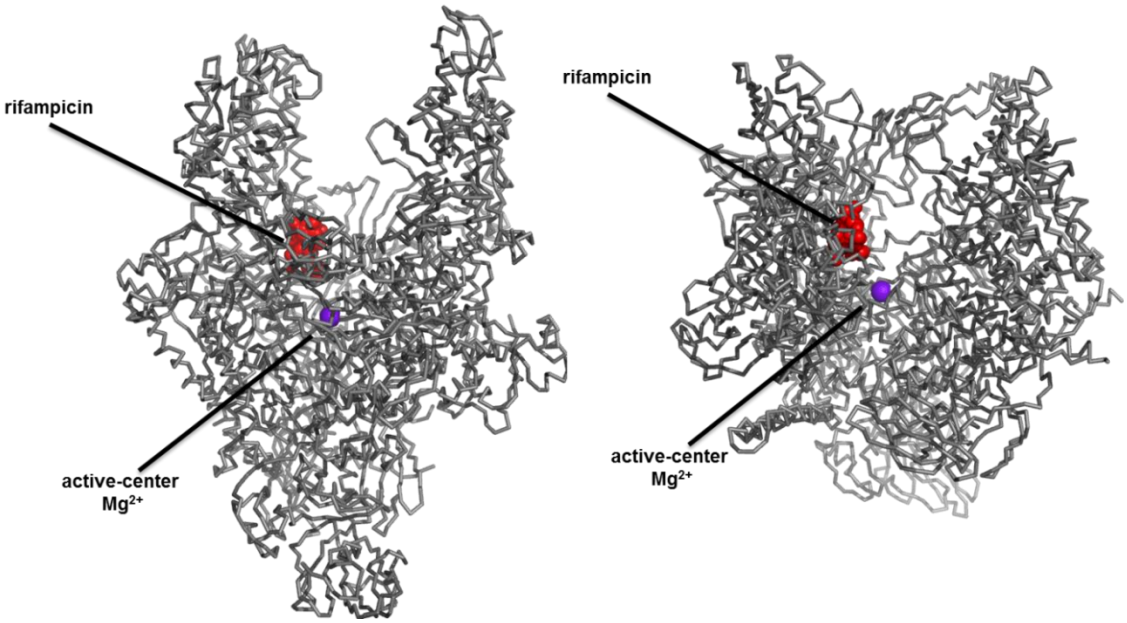

Figure 4: Location of rifampicin target within bacterial RNAP.

Thermus *aquaticus* core bound with rifampicin at 3.3 Å. Rifampicin is shown in red. The co-ordinates are taken from PDB accession code 1I6V.

A) Upstream view B) Top view

Through both structural and genetic studies it is determined that the β subunit residues 516 D, 526 D and 531 S (conserved in bacteria) are important for rifampicin binding [93, 94, 96]. Mutation in these three positions exhibits high level resistance to the rifampicin diminishing its clinical utility [97].

Rifamycins plays very important role as a first line drug in tuberculosis (TB) treatment, the introduction of rifamycins decreased the course of the treatment from 18-24 moths to 6-9 months [15]. Rifamycins are very potent inhibitors of *M. tuberculosis*, and can kill the bacilli in non-replicating or dormant state (which is highly desirable in TB treatment) [91, 98].

Rifamycins as a drug have some drawback, foremost is the emergence of rifamycin-resistant *M. tuberculosis*. The resistance rate is ~1X10^{-8}, and three of the frequently emerging mutants are substitution in the β residues 516 D, 526 D and 531 S (97% chance) [89, 96]. The emergence and dispersion of drug-resistant TB has threatened the clinical utility of rifamycin class of compounds in TB treatment [99-101]. Also, rifampicin induces increased expression of hepatic CYP (cytochrome P450 oxidase) [102]. The increase level of CYP decreases the therapeutic concentration of other drugs [103] (Important in the case of HIV patients where TB is the secondary infection and requires taking other medication).

1.6.2 Myxopyronin:

Myxopyronin is a naturally occurring α-pyrone antibiotic (Figure 5A), it is produced by *Myxococcus fulvus Mf50* [104]. It is an inhibitor of bacterial RNAP and specifically targets the switch region of RNAP. The myxopyronin binding site is determined through genetic and structural studies. It is observed that myxopyronin binding determinants is located at the base of the β' pincer and are the switch region 1 and switch region 2-sub-region [14]. Through biochemical studies it is established that myxopyronin interferes in the formation of RP_o [14]. Recently, through single molecule study it is determined that Myxopyronin interferes with the clamp closing [29]. Myxopyronin is a broad-spectrum antibiotic and inhibits RNAP and growth of both of Gram-positive and Gram-negative bacterial species [105].

1.6.3 CBR703:

CBR703 is an *E*. *coli* RNAP specific inhibitor (Figure 5B), it does not affect RNAP from Gram-positive bacteria or human RNAP [106, 107]. It is a synthetic lead compound isolated in 2001 through high-throughput screening performed against *E*. *coli* RNAP. It binds at a surface exposed surface, located at the junction of bridge helix and β subunit. CBR703 binding target does not overlap with RNAP active center, it is an allosteric inhibitor of Gram-negative bacterial RNAP. Through a series of biochemical experiment it was verified that CBR703 interferes with the nucleotide addition cycle, possibly by interfering with the conformational dynamics of the bridge helix [106].

Through lead optimization more potent analog of CBR703 was identified, with increased potency against *E*. *coli* RNAP [106].

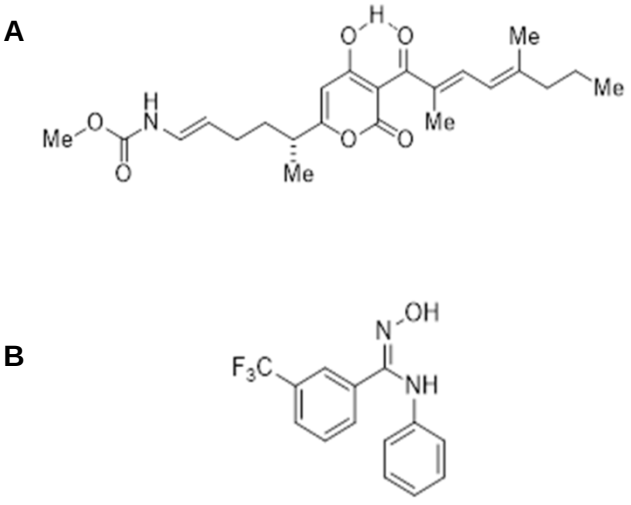

Figure 5: Structure of bacterial RNAP inhibitors

A) Structure of myxopyronin
B) Structure of CBR703

1.7 Mycobacterium

1.7.1 *Mycobacterium tuberculosis*:

Mycobacterium tuberculosis is pathogenic bacteria and the causative agent of tuberculosis (TB). It is a non-motile, rod shaped, obligate aerobe and can survive only in host tissue. *M*ycobacterium *tuberculosis* is a slow growing bacillus with typical doubling time of ~24 hours [108]. *M. tuberculosis* together with other tuberculosis causing mycobacteria (*M. bovis, M. africanum, M. caprae* etc.) belongs to a group called as *Mycobacterium tuberculosis* complex (MTBC) [109].

Mycobacterium tuberculosis H37Rv is a strain of *M. tuberculosis* isolated in 1905, it is widely used as a research strain as it has retained its virulence property and it is susceptible to drugs [108]. The entire genome of *M. tuberculosis* H37Rv is sequenced in 1998 and sequence information is available for all five RNAP subunits as well as sigma factor [108]. *M. tuberculosis* H37Rv contains thirteen sigma factors with σ^A as the primary sigma factor [110]. So far, there is no structural information available for Mycobacterium RNAP.

In our lab *Mycobacterium tuberculosis* RNAP genes were cloned into expression vector and highly pure and active recombinant *M. tuberculosis* RNAP holoenzyme capable of *in-vitro* transcription assay was successfully purified. (unpublished work).

Mycobacterium tuberculosis is generally resistant to many antibiotics. The resistance arises due to their extremely hydrophobic cell envelope which acts as barrier to many antibiotics [108]. The bacilli can achieve drug resistance through spontaneous

chromosomal mutation [111]. Another mechanism by which *Mycobacterium tuberculosis* can achieve antibiotic resistance is by attaining dormancy or a non-replicating state (a state of minimal cellular metabolism), these bacilli are called persisters [108, 112]. Rifamycin class of compounds are extremely potent in killing *Mycobacterium tuberculosis* and exhibits extremely low MIC (Minimum inhibitor concentration) [91]. *M. tuberculosis* can be cultured in laboratory condition both in liquid and agar based media. In laboratory it can be handled under biosafety level 3 (BSL3) condition.

1.7.2 Mycobacterium *tuberculosis* H37Rv mc^{2}6230

Mycobacterium tuberculosis H37Rv mc^{2}6230 is an engineered attenuated pantothenic acid auxotrophic mutant of *Mycobacterium tuberculosis* H37Rv (Vaccine strain).[113] This strain has a double deletion mutation of *panCD* gene and *RD1* gene. In bacteria pantothenic acid is synthesized from amino acid intermediate and *panC* and *panD* genes are required for de novo synthesis of pantothenic acid, deletion of these genes makes *Mycobacterium tuberculosis* H37Rv mc^{2}6230 strain pantothenic acid auxotroph and can resume normal growth only when supplemented with pantothenic acid. In addition it also has mutation in RD1 (region of difference 1) gene, which is known as responsible for *Mycobacterium tuberculosis* virulence. Thus, these two un-linked, non-reverting mutations makes *M. tuberculosis* H37Rv mc^{2}6230 an attenuated, non-virulent strain. As a result of the mutations *M. tuberculosis* H37Rv mc^{2}6230 is considered safe to be handled under BSL-2 regulated laboratory condition [113, 114]. This strain does not have any alteration in the RNAP genes *rpoB, rpoC, rpoA, rpoZ*, or *sigA*.

1.7.3 *Mycobacterium smegmatis*

Mycobacterium smegmatis is a fast-growing, non-pathogenic relative of *Mycobacterium*. *tuberculosis* [115]. It has a doubling time of 4 hours and forms colonies in about 2-3 days. *Mycobacterium smegmatis and Mycobacterium tuberculosis* RNAP coding genes, share more than 90% sequence identity. The fact that *Mycobacterium smegmatis* is fast growing and non-virulent, makes it easy to handle under laboratory conditions and also, together with the fact that it shares extensive RNAP gene sequence identity with *Mycobacterium tuberculosis*, makes *Mycobacterium smegmatis* an ideal candidate as a model organism substitute for *M*. *tuberculosis* in our study. The *Mycobacterium smegmatis* strain used in this study is *Mycobacterium smegmatis* ATCC19420.

1.8 Tuberculosis:

Human tuberculosis (TB) is a disease caused by *Mycobacterium tuberculosis* infection, mainly in the respiratory system. It is a contagious disease and can spread from human-to-human through bacilli suspended in air droplets (cough, sneeze etc.). In 1993 WHO (World Health Organization) declared TB as a global public health emergency. It ranks as the second leading cause of death from infectious disease the estimated mortality rate of TB in 2012 is 1.2 million [116]. Most of the TB incidence occurs in south-east Asia (58 %) and Africa (27%), and are the high burden countries (HBC) for the disease. The WHO estimates that about one third of the world population is infected with *M*.

tuberculosis and small population of the people infected with *Mycobacterium tuberculosis* develops TB and for majority of us the bacteria can remain dormant [116].

Latent TB is caused when the bacillus attains a dormant state in the infected tissue due to the host immune system. In such a state the growth or reproduction of the bacillus is controlled but not eradicated. Unlike TB, latent TB is not infectious and does not produce any symptoms. The bacillus can survive in the host tissue for years and can revert to active form producing the disease when the immune system is weak or compromised due to other infection or disease [117]. Two drugs rifamycins and pyrazinamide are known to clear latent TB infection [118, 119].

One of the contributing factors in resurgence of TB is the co-infection amongst HIV positive. The TB bacillus becomes active for people living with HIV (immunocompromised), and is a major cause of death with co-infection [120]. In year 2012 it is estimates about 8.6 million people have TB out of which 1.1 million cases are people who are co-infected with HIV The estimated mortality rate of TB in 2012 is 1.2 million out of which 320 000 is amongst HIV positive people. TB cases with HIV co-infection are very high in the African countries [116]. TB cases with co-infection with HIV poses a problem in treatment as one of the primary line antibiotic (Rifampicin) induces increased level of hepatic cytochrome (CYP) P450 oxidase and enhanced CYP level results in increased metabolism of co-medication or medication required to control HIV [103, 121].

The first effective chemotherapy is the drug “streptomycin”, discovered by Dr. Selman Waksman in 1940, at Rutgers University [122]. Since then various other drugs were introduced for TB treatment. Some of the most effective drugs used as primary line antibiotic for TB treatment are rifamycins, isoniazid, pyrazinamide and ethambutol.

Amongst these four antibiotics rifampicin and pyrazinamide targets and disinfects latent TB.

Current tuberculosis treatment requires very long and complex antibiotic regimen, current regimen requires intake of combination of drugs for 6 –7 months. Drug susceptible-TB treatment requires consumption of the four primary line antibiotics for 2 months followed by intake of rifamycins and isoniazid for additional 2 months [116, 123]. Since, TB treatment is long and complex; this post a problem of not completion of antibiotic course which in turns lead to remission of the disease and or emergence of drug-resistance.

TB is further complicated by the emergence of the drug-resistant TB, their prevalence and difficulty in detection.[124] Drug resistant TB is categorized in two forms 1) Multi-drug resistant or MDR-TB is resistant to two of the primary line antibiotic (rifampicin and isoniazid) and 2) extensively-drug resistant XDR-TB when it is resistant to the primary line antibiotics plus one or more secondary line antibiotic.[99, 125, 126] According to 2012 WHO TB report ~450 000 people developed MDR-TB and the estimated mortality is 170 000 (which is the mortality rate is ~37%) [116].

In the current scenario, TB treatment requires urgent attention and to begin with requires search for new antibiotic for treatment. Antibiotic with properties that can solve one or more problem arising in TB treatment like the long and complicated drug regimen, potent sterilizing effect on persisters and combatting drug resistance TB [116, 124].

1.9 High-throughput screening:

1.9.1 Initial screen

In 2009-2010 in collaboration with Global alliance for TB drug development and Dr. Edinson Lucumi and Dr. Scott Diamond at University of Pennsylvania an extensive High-throughput screen was performed with *Mycobacterium tuberculosis* RNAP-σ^A holoenzyme. Gram quantity of the enzyme was prepared and *in-vitro* fluorescent transcription assay was performed in which primary screen of 114,260 compounds for inhibition of *Mycobacterium tuberculosis* σA RNAP was performed out of which 189 hits (167 hits, excluding known RNAP inhibitors and known DNA binding compounds)

Secondary screen of 167 compounds for inhibition of *Mycobacterium tuberculosis* RNAP was performed out of which 88 were confirmed hits.

1.9.2 Hit characterization

Radiochemical assay was performed for the 66 obtainable hits for inhibition of *Mycobacterium tuberculosis* RNAP out of which, 39 compounds inhibited *Mycobacterium tuberculosis RNAP (*IC50 ≤ 50 μM (0.06-50 μM). Radiochemical assay was performed for the 39 re-confirmed hits to assess their action on inhibition of *E. coli* RNAP out of which, 24 (62%) inhibit *E*. *coli* RNAP; IC50 ≤ 50 μM (0.09-50 μM). MABA-MIC assay

was performed for 39 re-confirmed hits for activity against *M. tuberculosis* in culture. 15 (38%) inhibit *M. tuberculosis in culture*; MIC ≤ 50 µg/ml (0.78-50 µg/ml).

4 inhibit both *M. tuberculosis* RNAP and *E. coli* RNAP.

11 inhibit *M. tuberculosis* RNAP but not *E. coli* RNAP.

Out of the fifteen top hit compounds two compounds had the same scaffold.

1.9.3 AAP1:

AAP1 or N-α-benzoyl-N-(2-methylphenyl)-phenylalaninamide (Figure 6) is one of the top hit compounds identified through the high-throughput screening. AAP1 is a small molecule with mw 358.4 g/mol, it is a synthetic compound, and can be easily synthesized. AAP1 possess a chiral center, for all experimental purpose D/L-AAP1 was used unless mentioned. The D/L form can be easily resolved into D-AAP1 an L-AAP1 using chiral chromatography.

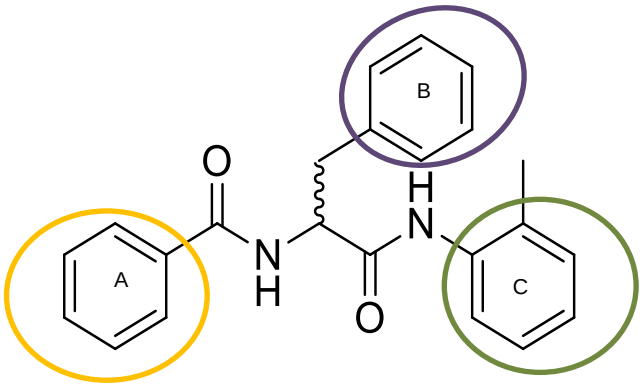

Figure 6: Structure of D/L AAP1 (N-α-benzoyl-N-(2-methylphenyl)-phenylalaninamide)

AAP1 in initial hit characterization assay exhibited potent *Mycobacterium tuberculosis* RNAP inhibitory effect and also antimycobacterial activity in growth inhibition assay. It does not exhibit any inhibitory effect on eukaryotic RNAP and on mammalian cell. AAP1 has a modular structure; it comprises three aromatic rings “A”, “B” and “C” connected via amide bonds. These three rings are amenable to parallel synthesis of analogs for hit-to-lead studies." "AAP1 offers exceptional promise as a lead for development of anti-tuberculosis drug.

In this study we have used an AAP1 analog “AAP12” which contains a single substituent of“4-hydroxy” in ring “B” of the parent compound. AAP12

3. AAPs: RNAP inhibitory activity and antibacterial activity

AAP1 was identified through high-throughput screening performed against *M. tuberculosis* RNAP. To assess the effect of AAPs (AAP1 and AAP12) on bacterial RNAP we performed *in-vitro* fluorescent transcription assays and determined the effect of AAPs on RNAP from *E. coli, S. aureus* and *M. tuberculosis*.

To assess the effect of AAPs on bacterial growth, we performed MIC (Minimum inhibitory concentration) assays. We have determined the effect of AAPs on growth of *E*. *coli*, *S*. *aureus* and *M*. *tuberculosis*, *M*. *smegmatis* and various other slow-growing Mycobacterium species.

Since AAP1 possess a chiral center, to assess the effect of each stereoisomer and identify the active isomeric form, we have determined the effect of D-AAP1 and L-AAP1 on mycobacterial RNAP and mycobacterial growth.

3.1 Materials and method:

3.1.1 List of plasmid in this work:

Plasmid	characteristics	source
pCOLADuet Mt rpoB-rpoC	ori-COLA; Kan^R; rpoB,	
pACYCDuet Mt rpoA (H10)	ori-P15A; Chl^R; (H10)-rpoA	
pCDFDuet Mt rpoZ	ori-CDF; str^R; rpoZ	
pET Mt sigA (H6)	ori-colE1; Kan^R; (H6)-sigA	
pCOLADuet Mt rpoBR553C-	ori-COLA; Kan^R; rpoB,	
pCOLADuet Mt rpoB-	ori-COLA; Kan^R; rpoB,	

Plasmid pCOLADuet Mt rpoB-rpoC, encodes β and β' subunits of *M. tuberculosis*. RNAP, under T7 promoter. Plasmid pACYCDuet Mt rpoA (H10) encodes decahistidine tagged M. *tuberculosis*. RNAP α subunit under T7 promoter. Plasmid pCDFDuet Mt rpoZ

encodes ω subunit of *M. tuberculosis*. RNAP. Plasmid pET Mt sigA (H6) encodes hexahistidine tagged σ^A subunit of *M*. *tuberculosis*. RNAP.

3.1.2 Preparation of *Mycobacterium tuberculosis* RNA polymerase core:

E. coli strain BL21DE3 was co-transformed with plasmid pCOLADuet-MtrpoB-rpoC, pACYCDuet-MtrpoA(H10)A, and pCDFDuet-MtrpoZ, colonies were selected in LB agar plate containing 100mg/ml kanamycin, 100mg/ml chloramphenicol, and 100 mg/ml streptomycin. Single colony was grown overnight in 100 ml 4XLB, which was transferred to 2.8 L fermenter minifors bench top bioreactor (infors HT). In fermenter cells were induced with 1mM IPTG when OD reached 4.0 at 600nm. Following IPTG induction cells were grown for 3-4 hours and harvested by centrifugation at (5000g for 20 mins at 4 °C). Cells were lysed using Avestin EmulsiFlex-C5 cell disrupter (Avestin Inc.) in lysis buffer containing 50mM Tris-HCl p H 7.9, 233 mM NaCl, 1mM DTT, 2mM EDTA, 5% glycerol and protease inhibitor cocktail tablets (Roche Inc.). The lysate was centrifuged at (20,000xg; 20 min at 4°C). The supernatant was collected to it 0.6-0.8% polyamine P was added, stirred at 4 °C for 10 min and centrifuged at 20,000xg; 15 min at 4°C. The pellet was washed three times with buffer containing 50 mM Tris-HCl pH 7.9, 5 mM DTT and 5% glycerol (TGD) with 500 mM NaCl After that the pellet was resuspended in TGD buffer containing 1 M NaCl, centrifuged at 20,000g for 15 min at 4°C, to the supernatant 30% ammoniumsulphate was added and stirred at 4°C for 20 mins, followed by centrifugation at 20,000 for 30 min at 4°C. The pellet was resuspended in buffer containing 50 mM Tris-HCl pH 7.9, 200 mM NaCl, 5 mM DTT and 5% glycerol it was loaded to Ni^{2+}- NTA column equilibrated with the same buffer, followed by washes with 5 column volume of same buffer containing no imidazole, 10 mM imidazole, 40 mM imidazole and protein was eluted with 250 mM imidazole. The eluted protein fraction were purified by 16/10 mono-Q (GE Healthcare Inc.) anion exchange chromatography

160 ml linear gradient of 200-500 mM NaCl in 50 mM Tris-HCl, pH 8.0, 1 mM dithiothreitol, and 5% glycerol; flow rate = 1 ml/min). Fractions containing *M. tuberculosis* RNAP core enzyme (~400 mM NaCl) were pooled and concentrated using 30 kDa MWCO Amicon Ultra-15 centrifugal ultrafilters (Millipore, Inc.), and were stored in 50 mM Tris-HCl, pH 8.0, 400 mM NaCl, 1 mM dithiothreitol, 5% glycerol at -80°C.

3.1.3 Purification of *Mycobacterium tuberculosis* σ^A:

Plasmid pET-MtsigA encoding hexahistidine tagged *M. tuberculosis* σ^A was transformed in E. *coli* strain BL21DE3 and colonies were selected in LB agar plate containing 100mg/ml ampicillin. Single colony was inoculated in 100 ml LB containing 100 mg/ml ampicillin grown overnight it was then transferred to 2 L LB and grown at 37 °C , cells were induced with 1mM IPTG when OD reached 0.4 and then grown at 16 °C for 12 hours. Cells were harvested at 5000 rpm for 20 min. The pellet were resuspended in lysis buffer containing (50 mM Tris-HCl, pH 8.0, 300 mM NaCl, 5 mM DTT and 5% glycerol with protein inhibitor tablet (Roche Inc)) and lysed using Avestin EmulsiFlex-C5 cell disrupter (Avestin Inc.) centrifuged at 20000 g at 4 °C for 30 min. The supernatant was loaded onto Ni^{2+}-NTA column equilibrated with lysis buffer. The column was washed with 5 Column volume of lysis buffer containing no imidazole 10 mM imidazole, 50 mM imidazole and eluted with lysis buffer containing 200 mM imidazole. The eluted protein was diluted with lysis buffer to NaCl concentration of 200 mM NaCl and was purified through anion exchange 16./10 mono Q (GE Healthcare Inc.) 160 ml linear gradient of 200-500 mM NaCl in 50 mM Tris-HCl, pH 8.0, 1 mM dithiothreitol, and 5% glycerol; flow rate = 1 ml/min). Fractions containing *M. tuberculosis* σ^A enzyme (~350 mM NaCl) were pooled, were concentrated using 30 kDa MWCO Amicon Ultra-15 centrifugal ultrafilters (Millipore, Inc.), and were stored in 50 mM Tris-HCl, pH 8.0, 400 mM NaCl, 1 mM dithiothreitol, 5% glycerol at -80°C.

3.1.4 BBT-ATP fluorescent *in-vitro* transcription assay: *Mycobacterium tuberculosis*

Reaction mixture (20 µl) contained 75 nM *M. tuberculosis* core RNAP and 300 nM *M. tuberculosis* σ_A in transcription buffer (40 mM Tris-HCl pH 8.0, 75 mM NaCl, 5 mM $MgCl_2$, 2.5 mM DTT, 12.7% glycerol) were incubated in ice for 10 mins, inhibitor at desired concentration was added and incubated at 37 °C for 10 min following that 20nM bacteriophage T5 N25 promoter DNA fragment was added and incubated for 5 min, then transcription was initiated by addition of rNTP mixture containing 100 µM GTP, 100 µM CTP, 100 µM UTP and 25 µM BBT-ATP, was incubated at 37 °C for 1 hr. The transcription reaction was measured as the amount of ATP incorporated in the reaction and release of BBT. After 1hr transcription was terminated by addition of 0.5M AMPSO and CIP (Calf alkaline phosphatase). Reaction mixture was transferred to 96 well plate (1/2 area flat bottom; corning 3686) and fluorescence emission was measured at 590 nm. For each reaction at least four concentrations of inhibitor was used and the IC_{50} values of each inhibitors were calculated by fitting the data in sigma plot hyperbolic single rectangular one parmeter.

3.1.5 BBT-P-CTP fluorescent *in-vitro* transcription assay: Bacterial RNAP

Reaction mixture (20 µl) contained 75 nM *E. coli* or *S. aureus* holoenzyme in transcription buffer (50 mM Tris-HCl pH 8.0, 100 mM KCl,10 mM $MgCl_2$, 1 mM DTT, 10 µg/ml BSA, 5 % glycerol), inhibitor at desired concentration was added and incubated at 37 °C for 10 mins following that 20nM bacteriophage T5 N25 promoter DNA fragment was added and incubated for 5 mins, then transcription was initiated by addition of rNTP mixture containing 100 µM GTP, 100 µM ATP, 100 µM UTP and 25 µM BBT-P-CTP, was incubated at 37 °C for 1 hr. The transcription reaction was measured as the amount

of ATP incorporated in the reaction and release of BBT. After 1hr transcription was terminated by addition of 0.5M AMPSO and CIP (Calf alkaline phosphatase). Reaction mixture was transferred to 96 well plate (1/2 area flat bottom; corning 3686) and fluorescence emission was measured at 590nm. For each reaction at least four different concentration of inhibitor was used and the IC_{50} values of each inhibitors were calculated by fitting the data in sigma plot hyperbolic single rectangular 2 parameter.

3.1.6 *Mycobacterium tuberculosis* H37Rv $mc^2$6230 MABA MIC assay (microplate alamar blue minimum inhibitory concentration assay):

Mycobacterium tuberculosis H37Rv $mc^2$620 was grown in 10 ml of Middlebrook7H9 broth (BD Inc.) supplemented with 0.5% (vol/vol) glycerol (Sigma Chemical), 10% (vol/vol) OADC (oleic acid, albumin, dextrose, catalase), 0.2% casamino acid, 24 µg/ml pantothenate and 0.05% (vol/vol) Tween 80 (Sigma) at 150 rpm and 37°C until they reach mid-log phase (optical density of 0.4 to 0.8 at 600 nm). Bacterial pellet was suspended in 10 ml PBS and to it 2ml, 5mm glass bead was added and vortex for 5-10 mins. The cell suspension was then passed through 8 µm filters, aliquot into vials and stored at -80 °C. From 3 random vials, 50 µl of cell suspension was diluted to 10^{-2} and 10^{-3} and was plated for cfu (colony forming unit) count after incubation at 37 °C for 15 days

200 µl of sterile deionized water was added to all outer-perimeter wells of sterile 96-well plates to minimize evaporation of the medium in the test wells during incubation. The wells in rows B to G in columns 3 to 11 received 100 ml of 7H9 broth (BD, Inc.) with Middlebrook OADC enrichment (BD, Inc.), 0.5% glycerol, 0.2% casamino acid, 24 µg/ml pantothenate and containing test compounds at 100 µg/ml. 100 µl of *M. tuberculosis*

H37Rv mc²6230 (frozen aliquot was adjusted to cfu $6X10^6$ with growth media) was added to the wells in rows B to G in columns 2 to 11. Each plate also contains cell only and media controls. The plates were sealed with parafilm and were incubated at 37°C for 7 days. On Day 7, 12.5 µl 20% Tween 80 and 20 µl Alamar Blue reagent (Invitrogen 10x ready to use reagent DAL1100) was added to the well containing cells and control wells. The plates were re-incubated at 37°C for 24 h and scored blue no growth, pink or violet as growth.

3.1.7 Determination of bacterial minimum inhibitory concentration (MIC) by broth dilution method:

MICs of *Mycobacterium smegmatis* ATCC19420, *E. coli* and *S. aureus* were quantified using broth microdilution assays as described. Clinical and Laboratory Standards Institute (CLSI/NCCLS) (2009) *Methods for Dilution Antimicrobial Susceptibility Tests for Bacteria That Grow Aerobically; Approved Standard, Eighth Edition. CLIS Document M07-A8* (CLIS, Wayne PA)].

For *Mycobacterium smegmatis* ATCC19420 MIC assays, Middlebrook SevenH9 media (BD Inc.) supplemented with Middlebrook ADC enrichment (BD Inc.), 0.5% glycerol and 0.05% tween80 was used.

3.2 Results and conclusion: RNAP inhibitory activity and antibacterial activity of AAPs

3.2.1 RNAP inhibitory activity

To determine the effect of AAPs on mycobacterial RNAP, fluorescent transcription assays were performed using fluorescent nucleotide analog γ-BBT-ATP (γ-[2'-(2-benzothiazoyl)-6'-hydroxybenzothiazole)-adenosine-5'-triphosphate). BBT is a fluorescent moiety with excitation at 422 nm and emission at 566 nm at pH ≥7.5 [127]. The IC_{50} value of AAP1 and AAP12 against *Mycobacterium tuberculosis* RNAP polymerase holoenzyme was determined to be ~2.9 μM and 5 μM respectively

To determine the effect of AAPs against bacterial RNAP from Gram-negative and Gram-positive organism we performed fluorescent transcription assay with *E*. *coli* and S. *aureus* RNAP. To do so fluorescent nucleotide analog BBT-P-CTP (γ-[2'-(2-benzothiazoyl)-6'-hydroxybenzothiazole)-cytosine-5'-tetraphosphate) was used as fluorescent CTP analog. The IC_{50} of AAP1 and AAP12 was determined to be >100 μM for both *E. coli* (Gram-negative) and *S. aureus* (Gram-positive) RNAP (Table 1).

The results of the transcription assays suggest that AAPs inhibits mycobacterial RNAP with much higher potency than RNAP from other bacterial species. Based on this observation we propose that AAPs inhibit mycobacterial RNAP potently and that AAPs are poor inhibitor or do not inhibit RNAP from *E coli* and *S. aureus.* Hence, we propose that AAPs inhibits mycobacterial RNAP with species specificity.

Table 1: Inhibition of bacterial RNAP: fluorescent in-vitro transcription assay

RNAP		AAP1 (μM)	AAP12 (μM)
Mycobacterial RNAP	*M. tuberculosis*	~2.9	~5.0
Gram-negative bacterial RNAP	*E. coli*	>100	>100
Gram-positive bacterial RNAP	*S. aureus*	>100	>100

To determine the effect of each AAP1 stereoisomer on M. *tuberculosis* RNAP, we performed *in-vitro* fluorescent transcription assay using isolated D-AAP1, L-AAP1 and compare the observation with D/L-AAP1. We observed that the IC_{50} of D-AAP1 was two-fold higher than D/L-AAP1 and that L-AAP1 inhibits mycobacterial RNAP very poorly with IC_{50} value >100 μM (Table 2).

Table 2: Inhibition of mycobacterial RNAP: AAP1 stereoisomers: fluorescent *in-vitro* transcription assay

Compound	IC_{50} (μM) fluorescent transcription assay
D/L-AAP1	2.9
D-AAP1	1.5
L-AAP1	>100

Thus the result suggests that D-isomeric form of AAP1 is responsible for the antimycobacterial RNAP activity and that L-isomeric form of AAP1 either does not inhibit mycobacterial RNAP poorly or poorly.

3.2.2 Antibacterial activity

To determine the effect of AAPs on *Mycobacterium tuberculosis* growth in liquid culture microplate alamar blue MIC assay (MABA MIC assay) was performed using *M. tuberculosis* H37Rv $mc^2$6230 (avirulent, pantothenate auxotroph derivative of *M. tuberculosis*). The MIC values of AAP1 and AAP12 for *Mycobacterium tuberculosis* H37Rv $mc^2$6230 were observed to be 6.25 µg/ml and 12.5 µg/ml (Table 3) respectively. We have also determined the MIC of AAP1 and AAP12 on various non-pathogenic, fast-growing mycobacterium sp. like *M. smegmatis*, *M. phlei* and *M. thermoresistible etc.* by broth microdilution method. We observed that AAPs inhibits the growth of *M. smegmatis* very efficiently at a concentration 16 fold (Table 3) less than *M. tuberculosis.* We also observed that AAPs did not affect the growth of other fast-growing thermophilic mycobacteria like *M. phlei*, *M. thermoresistible and M. hassiacum.* This differential growth inhibition can be attributed to either poor uptake of the compound or differential property of the efflux pump.

We have determined the effect of AAPs on growth of *Escherichia coli Df21tolc* (Gram-negative) and *Staphylococcus aureus* (Gram-positive) using broth dilution method and observed that AAP1 does not inhibit growth of either bacterium up to concentration of ≥ 50 µg/ml and AAP12 inhibited the growth of *Escherichia coli DH21f2Tolc* at a moderate

concentration of 12.5 µg/ml but did not affect the growth of *S. aureus* up to concentration of ≥50 µg/ml.

Thus results (Table 3) from the MIC assays suggest that AAPs inhibit the growth of mycobacterium efficiently and in a species specific manner.

Table 3: Minimum inhibitory concentrations (MIC) of bacterial growth in culture

Organism		**MIC AAP1 (µg/ml)**	**MIC AAP12 (µg/ml)**
Mycobacterium	*M. tuberculosis*	6.25	12.5
	M. smegmatis	0.39	0.39
	M. thermoresistibile	>50	12.5
	M. phlei	>50	12.5
	M. hassiacum	>50	>50
Gram-positive	*S. aureus*	>50	>50
Gram-negative	*E. coli DH21f2Tolc*	>50	12.5

To determine the stereoisomer specific activity of AAP1 we assessed the effect of isolated D-AAP1 and L-AAP1 on mycobacterial growth and compared the effect with that of D/L-AAP1. We observed that D-AAP1 exhibits twofold higher activity than D/L-AAP1 in mycobacterial growth inhibition and L-AAP1 did not inhibit the growth even at a concentration of ≥50 µg/ml (Table 4).

Table 4: Minimum inhibitory concentration (MIC) of mycobacterial growth in culture: AAP1 stereoisomers

Compound	**MIC (µg/ml)** ***M. smegmatis*** **ATCC19420**	**MABA MIC (µg/ml)** ***M. tuberculosis*** **H37Rv** **mc^{2}6230**
D/L-AAP1	0.39	6.25
D-AAP1	0.19	3.13
L-AAP1	50	>50

The MIC assay results are consistent with observation from transcription assays. Based on the observation from both mycobacterial RNAP inhibitory assays and mycobacterial growth inhibition assays, we propose that the D isomeric form of AAP1 is responsible for the antimycobacterial RNAP activity and antimycobacterial activity and that the L-isomeric form of AAP1 is either inactive or exhibit poor antimycobacterial activity.

4. Target of AAPs: *Mycobacterium tuberculosis* and *Mycobacterium smegmatis*

Since, AAPs are inhibitor of mycobacterial RNAP and mycobacterial cells our goal was:

1. To examine the role of RNAP as the functional cellular target of AAPs in mycobacteria (*M. smegmatis* and *M. tuberculosis).*

2 To identify and elucidate the AAP-binding target within bacterial RNAP (*M. smegmatis* and *M. tuberculosis).*

3. To determine resistance rate for AAP1 in *M. smegmatis* and compared that with resistance rate for rifampicin.

4. To determine the relationship between AAP-target and rifampicin-target in bacterial RNAP.

4.1 Materials and methods:

4.1.1 Isolation of AAP1-resistant *Mycobacterium smegmatis* ATCC19420 mutants:

Mycobacterium smegmatis ATCC 19420 ($0.7x10^9$-$2x10^9$ cfu/plate) were plated on Middlebrook Seven H11 agar base (BD, Inc.) containing Middlebrook ADC enrichment (BD, Inc.), 0.5% glycerol, and 1.56, 3.13, or 6.25 µg/ml of AAP1, and single colonies were isolated after 96 h at 37°C.

For each of the independent AAP1-resistant mutants, the *rpoB* gene encoding the RNA polymerase second-largest subunit, beta, and the *rpoC* gene encoding the RNA polymerase largest subunit, beta', were isolated and sequenced as follows: Cells were lysed using 10 mg/ml lysozyme (Sigma, Inc.). Genomic DNA was isolated using the

Wizard Genomic DNA Purification Kit (Promega), Inc.; procedures as specified by the manufacturer), and genomic DNA was quantified by measurement of UV-absorbance. The *rpoB* and *rpoC* genes were PCR-amplified in 50 μl reactions containing 50-200 ng genomic DNA, 0.5 μM forward and reverse oligonucleotide primers (5'-GTGCTGGAAGGATGCATCTTGGCAGT-3' and 5'-TTGCGGGACAGGTTGATTCCCAGGTTCGCG-3' for *rpoB*; 5'-GTGCTAGACGTCAACTTCTTCG-3' and 5'-TTAGCGGTAATCCGAGTAGCC-3' for *rpoC*), 25 μl 2x Phusion High-Fidelity PCR Master Mix with GC Buffer (New England Biolabs, Inc.) (initial denaturation step of 30 s at 98°C; 30 cycles of 10 s at 98°C, 30 s at 60°C for *rpoB* or 30 s at 55°C for *rpoC*, and 4 min at 72°C; final extension step of 10 min at 72°C). PCR products containing the *rpoB* gene (3.5 kB) or the *rpoC* gene (4.0 kB) were isolated by electrophoresis on 0.8% agarose, extracted from gel slices using the QIAquick Gel Extraction Kit (Qiagen, Inc.; procedures as specified by the manufacturer), and sequenced (Sanger sequencing; nine sequencing primers (Table SB1-SB9) for *rpoB* and ten sequencing primers (Table SC1-SC10) for *rpoC*).

4.1.2 Analysis of locations of AAP1-resistant mutants within structure of RNA polymerase

Sites of substitutions conferring AAP1-resistance (Table 6) were mapped onto the crystal structure of *Thermus thermophilus* RNA polymerase holoenzyme (PDB accession code 1L9U [Vassylyev, D., Sekine, S., Laptenko, O., Lee, J., Vassylyeva, M., Borukhov, S., Yokoyama, S. (2002) Nature, 417, 712-719]). Correspondences between residues of *Mycobacterium smegmatis* RNA polymerase and *Thermus thermophilus* RNA polymerase were based on amino acid sequence alignments [Lane, W., Darst, S. (2010) J. Mol. Biol. 395, 671-685].

4.1.3 Level of AAP1 and AAP12 resistance in AAP1-resistant *Mycobacterium smegmatis* ATCC19420 derivative:

Level of AAP1 and AAP12 resistance was measured by broth dilution method with *M.* smegmatis ATCC19420 derivative as in (materials and method).

4.1.4 AAP1 spontaneous resistance rate: *Mycobacterium smegmatis* ATCC19420

Resistance rates were determined using fluctuation assays [Luria, S., Delbrück, M. (1943) *Genetics* 28, 491-511.]. Defined numbers of cells of *Mycobacterium smegmatis* ATCC 19420 ($0.7x10^9$-$2x10^9$ cfu/plate) were plated on Middlebrook Seven H11 agar base (BD, Inc.) containing Middlebrook ADC enrichment (BD, Inc.) and 0.5% glycerol, and also containing 2xMIC, 4xMIC, or 8xMIC of test compound on this medium (1.56, 3.13, or 6.25 µg/ml for AAP1), and numbers of colonies were counted after 96 h at 37°C (at least 3 independent determinations for each concentration of each test compound). Resistance rates and 95% confidence intervals were calculated using the Ma-Sandri-Sarkar Maximum Likelihood Estimator (MSS-MLE [Ma, W., Sandri, GvH., Sarkar, S. (1992.) *J. Appl. Probab*. 29, 255-267; Sarkar, S., Ma, W., Sandri, GvH. (1992) *Genetica* 85, 173-179]) [128] as implemented on the Fluctuation Analysis Calculator (FALCOR; http://www.keshavsingh.org/protocols/FALCOR.html [Hall, B., Ma, C., Liang, P., Singh, K (2009) *Bioinformatics* 25, 1564-1565]) [129]. Sampling correction was performed as in [Stewart, F., Gordon, D., Levin, B. (1990) *Genetics* 124, 175-185 [130]; Jones, M. (1993) *Mutat. Res.* 292, 187-189 [131].

4.1.5 Rifampicin spontaneous resistance rate: *Mycobacterium smegmatis* ATCC19420

Resistance rates were determined using fluctuation assays [Luria, S., Delbrück, M. (1943) *Genetics* 28, 491-511.]. Defined numbers of cells of *Mycobacterium smegmatis* ATCC 19420 (~10^8 cfu/plate) were plated on Middlebrook Seven H11 agar base (BD, Inc.) containing Middlebrook ADC enrichment (BD, Inc.) and 0.5% glycerol, and also containing 8xMIC of test compound on this medium (50 µg/ml for rifampicin), and numbers of colonies were counted after 96 h at 37°C (at least six independent determinations for each concentration of each test compound). Resistance rates and 95% confidence intervals were calculated using the Ma-Sandri-Sarkar Maximum Likelihood Estimator (MSS-MLE [Ma, W., Sandri, GvH., Sarkar, S. (1992.) *J. Appl. Probab*. 29, 255-267; Sarkar, S., Ma, W., Sandri, GvH. (1992) *Genetica* 85, 173-179]) [128] as implemented on the Fluctuation Analysis Calculator (FALCOR; http://www.keshavsingh.org/protocols/FALCOR.html [Hall, B., Ma, C., Liang, P., Singh, K (2009) *Bioinformatics* 25, 1564-1565]) [129]. Sampling correction was performed as in [Stewart, F., Gordon, D., Levin, B. (1990) *Genetics* 124, 175-185 [130]; Jones, M. (1993) *Mutat. Res.* 292, 187-189 [131].

4.1.6 Isolation of AAP12-resistant *Mycobacterium tuberculosis* H37Rv mc^{2}6230:

M. tuberculosis H37Rv mc^{2}6230 (~10^9 cfu/plate) were plated on Middlebrook Seven H11 agar base (BD, Inc.) containing Middlebrook OADC enrichment (BD Inc.), 0.5% glycerol, 0.2% casaminoacid (BD Inc.),100 µg/ml pantothenate, and 3.13, or 6.25 µg/ml, 12.5 µg/ml, of AAP12, and single colonies were isolated after 15 days incubation at 37°C.

For each of the independent AAP12-resistant mutants, the *rpoB* gene encoding the RNA polymerase second-largest subunit, beta, and the *rpoC* gene encoding the RNA

polymerase largest subunit, beta', were isolated and sequenced as follows: Cells were lysed using 10 mg/ml lysozyme (Sigma, Inc.). Genomic DNA was isolated using the Wizard Genomic DNA Purification Kit (Promega), Inc.; procedures as specified by the manufacturer), and genomic DNA was quantified by measurement of UV-absorbance. The *rpoB* and *rpoC* genes were PCR-amplified in 50 μl reactions containing 50-200 ng genomic DNA, 0.5 μM forward and reverse oligonucleotide primers (5'- ATG GTG TTG GCA GAT TCC CGC CAG AG -3' and 5'- TTA CGC AAG ATC CTC GAC ACT TGC CC -3' for *rpoB*; 5'- GTG CTC GAC GTC AAC TTC TTC GAT GA -3' and 5'- CTA GCG GTA GTC GCT GTA GCC GTA GT -3' for *rpoC*), 25 μl 2x Phusion High-Fidelity PCR Master Mix with GC Buffer (New England Biolabs, Inc.) (initial denaturation step of 30 s at 98^{o}C; 30 cycles of 10 s at 98^{o}C, 30 s at 60^{o}C for *rpoB* or 30 s at 55°C for *rpoC*, and 4 min at 72^{o}C; final extension step of 10 min at 72^{o}C). PCR products containing the *rpoB* gene (3.5 kB) or the *rpoC* gene (4.0 kB) were isolated by electrophoresis on 0.8% agarose, extracted from gel slices using the QIAquick Gel Extraction Kit (Qiagen, Inc.; procedures as specified by the manufacturer), and sequenced (Sanger sequencing; nine sequencing primers for *rpoB* (Table B1-B9) and ten sequencing primers (Table C1-C10) for *rpoC*)

4.1.7 Level of AAP resistance for AAP-resistant *Mycobacterium tuberculosis* H37Rv mc^{2}6230 mutants:

AAP1 and AAP12 resistance level for AAP12-resistant *M. tuberculosis* H37Rv mc^{2}6230 mutants was determined by MABA MIC assay for each derivative. (As method 3.1.6)

4.1.8 *In-vitro* transcription assay for AAP-resistant *Mycobacterium tuberculosis* RNAP

Site-directed mutagenesis (Quick change II; stratagene Inc.) was performed to create plasmid pCOLADuet Mt rpoBR558C-rpoC and pCOLADuet Mt rpoB-rpoCI850S.

Plasmid pCOLADuet Mt rpoBR553C-rpoC produces RNAP with R→C substitution in RNAP β subunit. pCOLADuet Mt rpoB-rpoCI850S produces RNAP with I→S substitution in RNAP β' subunit.

Transcription assay was performed as section 3.1.4

4.1.9 Level of rifampicin cross-resistance in AAP1-resistant *Mycobacterium smegmatis* ATCC19420 derivative:

Level of rifampicin cross-resistance in AAP1-resistant *M. smegmatis* ATCC19420 derivative was measured by broth dilution method**.** (As method 3.1.7)

4.1.10 Isolation of rifampicin-resistance *Mycobacterium smegmatis* ATCC19420 derivative:

For isolation of rifampicin-resistance *M. smegmatis* ATCC19420, ~ 10^8 cfu cells were plated 7H11 agar plate with 0.5% glycerol and ADC enrichment containing 50 µg/ml rifampicin, plates were incubated at 37 °C for 96 hours and single isolated colony was selected.

For each of the independent Rifampicin-resistant mutants, the *rpoB* gene encoding the RNA polymerase second-largest subunit, beta, were isolated and sequenced as follows: Cells were lysed using 10 mg/ml lysozyme (Sigma, Inc.). Genomic DNA was isolated using the Wizard Genomic DNA Purification Kit (Promega, Inc.; procedures as specified by the manufacturer), and genomic DNA was quantified by measurement of UV-absorbance. The *rpoB* gene was PCR-amplified in 50 µl reactions containing 50-200 ng genomic DNA, 0.5 µM forward and reverse oligonucleotide primers (5'-GTGCTGGAAGGATGCATCTTGGCAGT-3' and 5'-TTGCGGGACAGGTTGATTCCCAGGTTCGCG-3' for *rpoB*, 25 µl 2x Phusion High-

Fidelity PCR Master Mix with GC Buffer (New England Biolabs, Inc.) (initial denaturation step of 30 s at 98^{o}C; 30 cycles of 10 s at 98^{o}C, 30 s at 60^{o}C for *rpoB* or 30 s at 55°C for *rpoC*, and 4 min at 72^{o}C; final extension step of 10 min at 72^{o}C). PCR products containing the *rpoB* gene (3.5 kB) was isolated by electrophoresis on 0.8% agarose, extracted from gel slices using the QIAquick Gel Extraction Kit (Qiagen, Inc.; procedures as specified by the manufacturer), and sequenced (Sanger sequencing; nine sequencing primers (Table SB1-SB9) for *rpoB*).

4.1.11 AAP1 cross-resistance level for rifampicin-resistance *M*ycobacterium *smegmatis* ATCC19420 derivative:

AAP1 cross-resistance level for Rifampicin-resistance *M. smegmatis* ATCC19420 mutants were determined by broth dilution method for each derivative.(As method 3.1.7)

4.1.12 Rifampicin, myxopyronin, lipiarmycin cross-resistance level for AAP12-resistant *Mycobacterium tuberculosis* H37Rvmc^{2}6230 mutants:

Rifampicin, myxopyronin and lipiarmycin cross-resistance level for AAP-resistant *Mycobacterium tuberculosis* H37Rv mc^{2}6230 mutant derivative was determined by MABA MIC method. (As method 3.1.7)

4.1.13 Primer-dependent transcription initiation assay: radiochemical *in-vitro* transcription assay

Reaction mixtures (8.1 ml) contained 40 nM *M. tuberculosis.* RNAP core and 120 nM σ^{A} (incubated on ice for 10 mins to form holoenzyme) or 40 nM E. *coli* RNAP holoenzyme, either none or one of antibiotics (10 mM and 40 µM of AAP1 and AAP12 respectively, 0.2 mM rifampicin, 40 mM CBR703), 40 mM Tris (pH 8.0), 75 mM NaCl, 5 mM $MgCl_2$, 2.5 mM DTT,12.5 % glycerol. Reaction mixtures were incubated at 37 °C for 10

minutes, supplemented with 0.5 ml 0.2 mM LacUV5-ICAP DNA, and incubated at 37 °C for 10 minutes. Reactions were initiated with 0.9 ml NTP subset (125 mM UTP, 0.1 µl of [α-32P]UTP 40mCi/ml, 5.6 mM ribodinucleotide ApA), and allowed at 37 °C for 10 minutes. Reactions mixtures were subsequently supplemented with 10 µl loading buffer (10 mM EDTA, 0.02% bromophenol blue, 0.02% xylene cyanol, and 80% formamide), nd boiled for 4 min at 95 °C Samples were applied to 15% polyacrylamide gels (19:1 acrylamide:bisacrylamide), electrophoresed in 90 mM Tris-borate (pH 8.0) and 2 mM EDTA, and analyzed by storage-phosphor scanning (Typhoon; GE Healthcare, Inc.).

4.2 Results and conclusion: Target of AAPs: *Mycobacterium smegmatis* and *Mycobacterium tuberculosis*

4.2.1 Identification of AAP target in *Mycobacterium smegmatis*:

To determine the functional cellular target of AAP1 in mycobacteria we used genetic approach of isolation of spontaneous resistant mutants. To begin with we used *M. smegmatis* ATCC19420 as representative mycobacteria, because of three primary reasons 1) it is fast growing compared to *M. tuberculosis*, 2) easy to handle is a BSL1 organism compared to *M. tuberculosis* (BSL2/BSL3) and 3) lower AAP1 MIC compared to *M. tuberculosis.*

To achieve so, high cfu (~10^9 cfu/plate) of *M. smegmatis* was spread on agar plate containing various concentrations of AAP1. Single isolated colonies arising after incubation at 37 °C for 96 h were re-streaked, followed by growing them in liquid media and genomic DNA isolation. *rpoB* (~3.5 kb) the second-largest subunit, and *rpoC* largest

subunit (~ 4kb) gene was PCR amplified. The PCR product was sequenced using overlapping primers and compared with *M*ycobacterium *smegmatis* wild-type *rpoB* and *rpoC* sequence.

A total of 19 independent AAP1-resistant mutants were isolated using the above method and characterized.

Table 5: AAP-resistant mutation in RNAP genes: *Mycobacterium smegmatis*

number of AAP-resistant isolates	19
number of AAP-resistant isolates containing mutation in *rpoB*	17
number of AAP-resistant isolates containing mutation in *rpoC*	2
Percentage of AAP-resistant isolates containing mutations in RNAP-subunit	100%

All 19 independent AAP1-resistant mutants were found to contain mutations in RNA polymerase genes *rpoB* or *rpoC* (Table 5). 17 contained mutations in the *rpoB* gene encoding RNA polymerase β subunit, and 2 contained mutations in the *rpoC* gene encoding RNA polymerase β ' subunit (Table 5). All nineteen AAP1-resistant mutants isolated were single-substitution mutants and 100% of the mutants isolated contained mutation in either *rpoB* or *rpoC* gene. The fact that 100% of spontaneous AAP1-resistant mutants map to RNA polymerase subunit genes indicates that RNA polymerase is the functional cellular target of AAP1 and indicates that inhibition of mycobacterial RNA polymerase by AAP1 accounts for inhibition of mycobacterial growth by AAP1.

Table 6: AAP resistant mutant: sequence: *Mycobacterium smegmatis*

amino acid substitution	number of independent isolates
***rpoB* (RNAP β subunit)**	
468 pro→Ser	1
470 His→Arg	2
477 Ile→Phe	1
553 Arg→Cys	2
553 Arg→Gly	1
553 Arg→Pro	1
557 Gly→Ser	3
559 Val→Gly	2
571 Asp→Gly	2
576 Gln→Arg	2
***rpoC* (RNAP β' subunit)**	
833 Arg→Gly	1
850 Ile→Ser	1

A total of 12 different substitutions conferring AAP1-resistance were identified (Table 6). These 12 substitutions, obtained are present at ten sites in *Mycobacterium smegmatis* RNA polymerase β subunit (residues 466, 470, 477, 553, 557, 571, and 576) and at 2 different sites in *Mycobacterium smegmatis* RNA polymerase β' subunit (residues 833 and 850) (Table 6). The results indicate that residues 466, 470, 477, 553, 557, 571, and 576 of *Mycobacterium smegmatis* RNA polymerase β subunit and

residues 833 and 850 of *Mycobacterium smegmatis* RNA polymerase β' subunit are important for inhibition of mycobacterial RNA polymerase and inhibition of mycobacterial growth by AAP1.

We quantified the level of AAP resistance for each of the AAP1-resistance M. *smegmatis* isolated by broth dilution method. The level of resistance was calculated based on the ratio of observed AAP MIC value of wild-type *M. smegmatis* over the MIC value of AAP1-resistant mutant derivative. All AAP1-resistant mutants were observed to exhibit at least ≥16 fold resistance to AAPs and ten mutants were observed to exhibit ≥ 60 fold resistances toward AAPs (Table 7). The fact that all AAP1-resistant mutant derivative exhibited resistance to AAPs is consistent with the fact that these amino acid residues are important for inhibition of mycobacterial growth by AAP.

Table 7: AAP-resistant mutant: sequence and property: *Mycobacterium smegmatis*

amino acid substitution	resistance level AAP1 (MIC/MIC$_{wild-type}$)	resistance level AAP12 (MIC/MIC$_{wild-type}$)
***rpoB* (RNAP β subunit)**		
468 pro→Ser	>16	>16
470 His→Arg	>16	≥60
477 Ile→Phe	>16	>60
553 Arg→Cys	>16	>60
553 Arg→Gly	>16	>60
553 Arg→Pro	>16	>60
557 Gly→Ser	>16	>60
559 Val→Gly	>16	>60
571 Asp→Gly	>16	>60
576 Gln→Arg	>16	>60
***rpoC* (RNAP β' subunit)**		
833 Arg→Gly	>16	≥60
850 Ile→Ser	>16	>30

4.2.2 Analysis of locations of AAP-resistant mutants within structure of RNA polymerase:

To analyze the location of AAP1-resistant mutants within structure of RNAP, the sites of substitutions conferring AAP1-resistance (Table 6) were mapped onto the crystal structure of *Thermus thermophilus* RNA polymerase holoenzyme (PDB accession code 1IW7 [Vassylyev, D., Sekine, S., Laptenko, O., Lee, J., Vassylyeva, M., Borukhov, S.,

Yokoyama, S. (2002) Nature, 417, 712-719] [32]). Correspondences between residues of *Mycobacterium smegmatis* RNA polymerase and *Thermus thermophilus* RNA polymerase were performed based on amino acid sequence alignments [Lane, W., Darst, S. (2010) J. Mol. Biol. 395, 671-685] [132].

In the three-dimensional structure of RNA polymerase, the ten sites of substitutions on *rpoB* gene and two sites of substitution on *rpoC* gene conferring AAP1-resistance, forms a tight cluster (the "AAP1 target"; Figure).

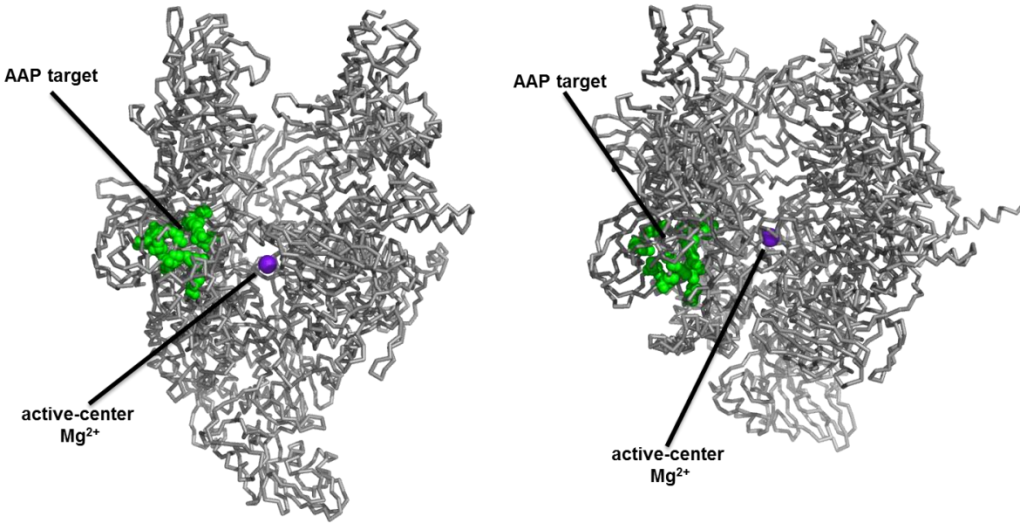

Figure 7: Location of AAP target within bacterial RNAP

In green are the amino-acid residues responsible for AAP-resistance, in purple Mg^{2+}. For clarity β' non-conserved region and σ subunit is removed. A) Upstream view B) Top view

Thermus thermophilus RNAP holoenzyme at 3.3 Å resolution. Atomic coordinates taken from PDB accession code: 1IW7

The dimensions of the AAP1 target are ~23 Å x ~23 Å x ~10 Å (Figure 2) and this AAP1 target is sufficiently large enough to be able to encompass AAP1 (~12 Å x ~8 Å x ~4 Å). Based on the resistance properties and the size of the AAP1 target, we propose that the AAP1 target is the binding site for AAP1 on RNA polymerase.

4.2.3 Rate of spontaneous resistance: *Mycobacterium smegmatis*

Spontaneous resistance rate for AAP1 in *M. smegmatis* ATCC19420 was determined by fluctuation assay. To do so, defined cfu of cells ~10^8-10^9 were plated on 7H11 agar plate containing 2x, 4x, 8x MIC of AAP1. The plates were incubated at 37 °C for 96 after that the number of single isolated colony arising on the plates were counted. Resistance rate was calculated based on MSS-MLE method [133] using four independent trials.

One of the mechanisms used by bacterium to achieve antibiotic resistance is spontaneous mutation in chromosomal DNA. Bacterial chromosome can accumulate spontaneous mutations (without antibiotic selection pressure or external mutagenic reagent) and it is a characteristic of the DNA polymerase error or mutations induced by endogenous agents. These mutations are changes in an organism's DNA which are inherited by the following generations. In this current section we have determined the rate of spontaneous resistant mutation to AAP1 in *M. smegmatis* ATCC19420. The rate of spontaneous mutation provides an estimate of the rate at which the amino acid residues responsible for binding with AAP can mutate and confer resistance to AAP1.

Table 8: AAP1 resistance rate: *Mycobacterium smegmatis*

AAP1 concentration	resistance rate/generation
spontaneous resistance rate at 2X MIC	$4x10^{-9}$
spontaneous resistance rate at 4X MIC	$5x10^{-9}$
spontaneous resistance rate at 8X MIC	$4x10^{-9}$

The results suggest that the mutation rate of AAP1 at 2x is $4X10^{-9}$, 4x is $5X10^{-9}$ and 8x is $4X10^{-9}$. The rate of spontaneous resistance for rifampicin at concentration of 50 µg/ml determined for *Mycobacterium smegmatis* ATCC19420 under identical condition was observed to be $6.3X10^{-9}$. Hence, the observed resistance rate for AAP1 is comparable or slightly lower to that of rifampicin resistance rate.

In TB treatment to diminish the emergence of antibiotic-resistant bacteria, combination therapy is used, in which more than one antibiotic is prescribed at a given time. Since the mutations are not linked, theoretically the probability of acquiring resistance to two drugs is the product of each resistance-rate (which is in case of AAP1 and rifampicin should be $4\text{-}5X10^{9}$ X $6X10^{9}$=24-30 ~10^{18}) [134]. We verify the fact that the rate of resistance when AAP1 and rifampicin will be used in combination will be greater than either antibiotic. To do so we examined the effect of combination of AAP1 and rifampicin in emergence of resistance mutants. To do so, we plated defined amount of cells 10^{8}-10^{9} on plates containing AAP1 (2X, 4X, 8X) and 50 µg/ml rifampicin. Total four trials were performed at each AAP1 concentration and no resistant mutant was observed (Total 12 independent trials were performed). The results suggest that the combination of AAP1 and rifampicin increases the rate of resistance than each inhibitor.

4.2.4 Identification of AAP target in *Mycobacterium tuberculosis*:

To demonstrate that the cellular target of AAP in *M. tuberculosis* a slow growing, pathogenic mycobacteria is identical with its fast growing non-pathogenic relative *M. smegmatis*, AAP-resistant spontaneous mutants of *M. tuberculosis H37Rv mc^{2}6230* were isolated and characterized (Table 9). To do so the AAP-resistant *M. tuberculosis* mutants were grown in liquid culture their genomic DNA isolated and *rpoB* (~3.5 kbp) and *rpoC* (~4 kbp) genes were PCR amplified and sequenced with over-lapping primers. A total of 4 independent AAP-resistant mutants were isolated and characterized (Table). All 4 independent AAP-resistant mutants were found to contain mutations in RNA polymerase *rpoB* gene encoding RNA polymerase β subunit. The fact that 100% of spontaneous AAP-resistant mutants map to RNA polymerase subunit genes indicates that RNA polymerase is the functional cellular target of AAP in *Mycobacterium tuberculosis.* It also indicates that inhibition of mycobacterial RNA polymerase by AAP accounts for inhibition of mycobacterial growth by AAP.

Table 9: AAP-resistant mutations in RNAP genes: *Mycobacterium tuberculosis*

number of AAP-resistant isolates	4
number of AAP-resistant isolates containing mutation in rpoB	4
number of AAP-resistant isolates containing mutation in rpoC	0
Percentage of AAP-resistant isolates containing mutations in RNAP-subunit	100%

A total of 4 different substitutions conferring AAP-resistance were identified (Table 9). Substitutions were obtained at distinct 3 sites in *Mycobacterium tuberculosis*

RNA polymerase β subunit (residues 473, 558 and 581). These three sites correspond exactly identically to previously isolated AAP1-resistant mutation sites in *M. smegmatis* (Table 10). The result corroborates the fact that the functional cellular target for AAP in mycobacteria is RNAP and also the fact that the residue 473, 558 and 581 are important for inhibition of mycobacterial growth by AAP, and forms the AAP target. This observation is consistent with the previous results from *Mycobacterium smegmatis* experiments.

Table 10: AAP-resistant mutant: sequence: Mycobacterium *tuberculosis*

amino acid substitution	number of independent isolates
***rpoB* (RNAP β subunit)**	
473 Pro→Thr=(468 in *M. smegmatis*)	1
558 Arg→Gly=(553 in *M. smegmatis*)	1
558 Arg→Ser=(553 in *M. smegmatis*)	1
581 Gln→Arg=(576 in *M. smegmatis*)	1

To verify the fact that the isolated AAP-resistant mutant M. *tuberculosis* is resistant to AAPs we have determined the level of AAP resistance for each of the AAP-resistant mutants *M. tuberculosis* isolated by MABA MIC. The level of resistance was calculated based on the ratio of the observed wild-type MIC over the MIC of the mutant derivative. The result indicates that the AAP-resistant mutant derivatives exhibit at least ≥2 fold resistance to AAPs. This result is consistent with previous observation (*M. smegmatis*) and also, confirms the importance of the involvement of these residues in inhibition of mycobacterial growth by AAPs.

Table 11: AAP-resistant mutant: sequence and property: *Mycobacterium tuberculosis*

amino acid substitution	resistance level (MIC/MIC$_{wild-type}$)	
	AAP1	AAP12
***rpoB* (RNAP β subunit)**		
473 Pro→Thr	>2	≥2
558 Arg→Gly	>2	>2
558 Arg→Ser	>2	>2
581 Gln→Arg	>2	>2

4.2.4.1 Transcription assay: AAP-resistant *Mycobacterium tuberculosis* RNAP derivative:

To confirm the direct involvement of the amino acid residue (isolated by sequencing spontaneous resistant mutants) as the binding determinant of AAP, two *Mycobacterium tuberculosis* RNAP derivatives containing mutation, β R558C in *rpoB* and β'I850C in *rpoC* was purified and in-vitro BBT-fluorescent transcription assay was performed

Site-directed mutagenesis was performed on "plasmid pCOLADuet MtrpoB-rpoC "to create plasmid having desired mutation in β (*rpoB)* or β' (*rpoC)* subunit of *M. tuberculosis*. RNAP.

Fluorescent *in-vitro* transcription assay was performed with each of the mutant enzyme and AAP1 IC_{50} was determined (Table 12). Level of resistance was calculated as the ratio of observed AAP1 IC_{50} of wild-type enzyme over AAP1-resistant mutant enzyme. Comparing the AAP1 IC_{50} value of mutant and wild-type enzyme indicates that the β subunit 553 R→C mutation confers >100 fold resistance to AAP1 (which is also observed in the AAP1 resistance level by broth dilution MIC and MABA-MIC). The IC_{50} value of β' subunit 850 I→S, when compared with that of wild-type IC_{50} value, indicates that this mutation confers ~ 3.5 fold resistance (which is also observed in the AAP1

resistance level by broth dilution MIC and MABA-MIC). The *in-vitro* transcription assay result is consistent with the previous result from spontaneous resistant mutants and confirms the direct involvement of these amino acid residues in conferring r AAPs.

Table 12: Resistance level *in-vitro* transcription assay:

Amino acid substitution	IC_{50} (μM) BBT-ATP fluorescent transcription assay	resistance level
None	2.9	1
rpoB R558C=(553 in *M*. *smegmatis*)	320	110
rpoC I851S = (850 in *M*. *smegmatis*)	10	3.4

4.2.5 Relation between AAP binding target and RNAP active center

Based on the amino acid determinants responsible for AAP-resistance, the inferred site of AAP binding within RNAP is at the base of the β lobe and N-terminal of the β' subunit bridge-helix. Analysis of the AAP target within RNAP indicates that, the binding target is distant from the RNA polymerase active center and does not exhibit any overlap with RNAP active center cleft, DNA binding determinants, RNA binding determinant or NTP entrance or binding determinant. Based on this absence of overlap we can infer that AAPs does not function through steric interaction with DNA, RNA or NTP interaction and that AAPs functions allosterically. Based on the location of AAP binding target we can also infer that AAP directly interacts with the RNAP β' subunit bridge helix and interferes with its conformational dynamic. From biochemical and crystal structure evidence it is known that RNAP bridge helix under goes conformation change in NTP addition cycle and translocation. Thus, we propose that AAP binding hold the bridge helix in a straight

conformation, and thus in directly affects the nucleotide addition cycle and or translocation.

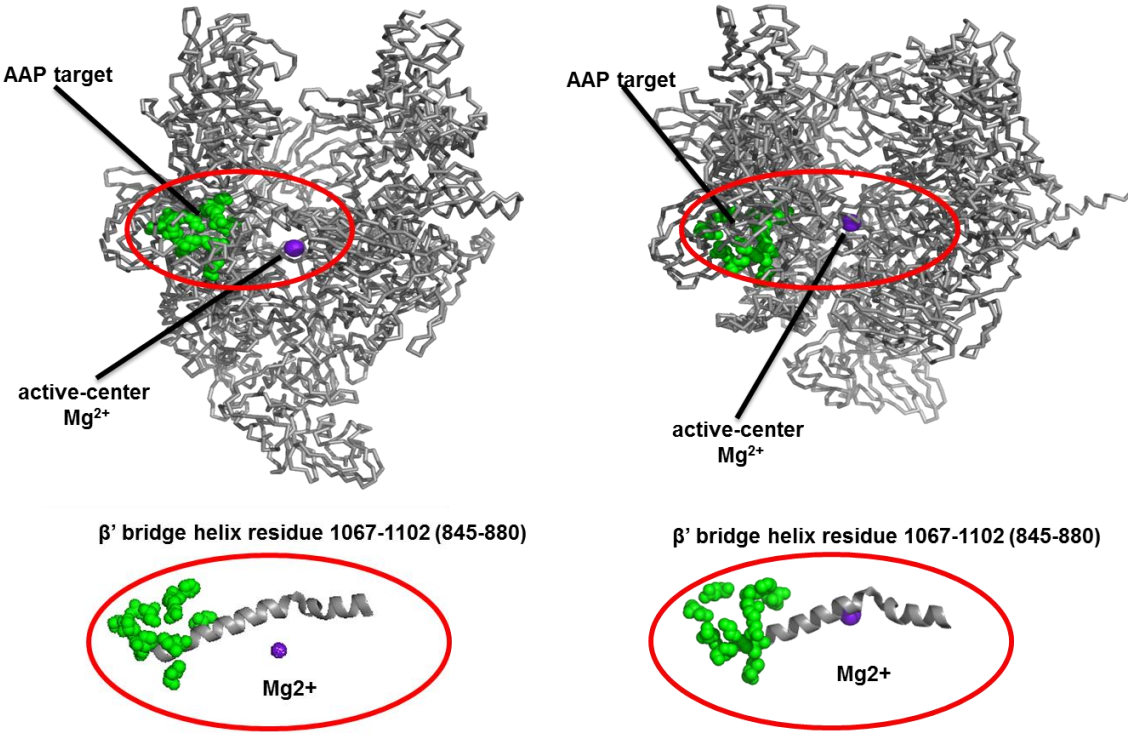

Figure 8: Location of AAP target within RNAP bacterial RNAP.

A) In green are the amino-acid residues responsible for AAP-resistance, in purple Mg^{2+}. For clarity β' non-conserved region and σ subunit is removed. View orientations are as in Figure

B) Stereo view of AAP binding region in context of β' bridge-helix. In green; are amino acid residues responsible for conferring AAP resistance, purple active-center Mg^{2+}. Residues are numbered as *T*. *thermophilus* RNAP and as in *M*. *smegmatis* RNAP in parenthesis.
Thermus thermophilus RNAP holoenzyme at 3.3 Å resolution. Atomic coordinates taken from PDB accession code: 1IW7

4.2.6 Relation of AAP and CBR703 target:

The binding target of AAP corresponds “essentially exactly” with “CBR703” an inhibitor of Gram-negative bacterial RNAP. The CBR703 target within *E*. *coli* RNAP was identified by using the approach of isolation of resistant mutants, (Ebright unpublished work) and it is observed to bind at the base of the β lobe and N-terminus of the β’ bridge helix. Thus, these two inhibitors bind at the exact same location within bacterial RNAP, but in species specific manner.

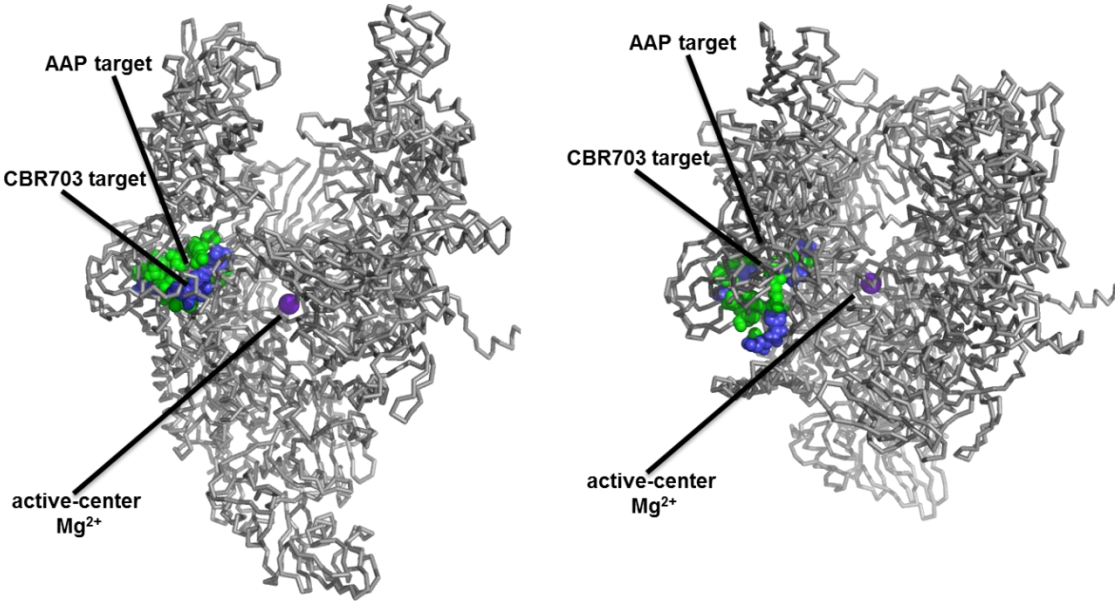

Figure 9: Location of AAP and CBR703 target within RNAP.

In green are the amino-acid residues responsible for AAP-resistance, in blue are amino-acid residue conferring CBR703 resistance (additional mutants which are not isolated in case of AAP), in purple Mg^{2+}. For clarity β’ non-conserved region and σ subunit is removed. View as in Figure: 7

Thermus *thermophilus* RNAP holoenzyme at 3.3 Å resolution. Atomic coordinates taken from PDB accession code: 1IW7

To determine the effect of AAPs and CBR703 on the RNAP from *M. tuberculosis* and *E. coli,* we performed a primer dependent transcription initiation assay. Since, CBR703 and AAPs both have identical target on bacterial RNAP, but in a species specific manner (which is CBR703 inhibit *E*. *coli* RNAP but does not inhibit *M*. *tuberculosis* RNAP in *in-vitro* transcription assay and vice versa up to a concentration of >100 µM). We examined, the effect of each those inhibitors in radiochemical *in-vitro* transcription initiation (primer-dependent) assay. To do so we used LacUV5 promoter (Figure 13) DNA and initiated the transcription reaction by addition of ApA primer and UTP, and examined the formation of ApApU* resolved in a 15% denaturing PAGE. (Figure 10)

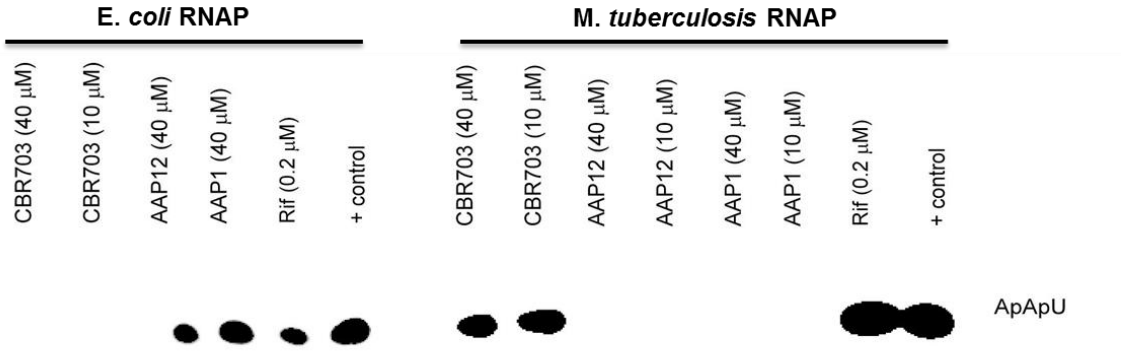

Figure 10: Effect of CBR703 and AAPs on *E. coli* and mycobacterial RNAP

Product resolved on 15% denaturing sequencing PAGE

In *E. coli* RNAP enzyme

+ Control contains no inhibitors and shows the formation of trinucleotide product, rifampicin, AAP1, AAP12 does not inhibit the formation of the trinucleotide product whereas CBR703 exhibits complete inhibitory effect.

In Mycobacterium *tuberculosis* RNAP

+ Control contains no inhibitors and shows the formation of trinucleotide product whereas rifampicin does not show inhibition. AAP1 and AAP12 in M. *tuberculosis* RNAP completely inhibit the formation of trinucleotide transcription product. CBR703 exhibits no or slight inhibition

In the above experiment we have observed that CBR703 at concentration of 10 µM and 40 µM completely inhibits the formation of ApApU product in *E*. *coli* RNAP but does not affect the formation of the same in Mycobacterium *tuberculosis* RNAP. We have observed a reciprocal effect with AAPs, which is AAPs, does not inhibit the formation of ApApU in transcription assay with *E*. *coli* RNAP and completely inhibits the formation of the product in *M*. *tuberculosis* RNAP even at 10 µM concentration. We have used rifampicin as the control; we observed that rifampicin does not affect the formation of ApApU for either *E*. *coli* or mycobacterial RNAP. The results suggest that AAPs are species specific inhibitor of mycobacterial RNAP and CBR703 for *E*. *coli* RNAP.

4.2.7 Relation of AAP and Rifampicin target:

The AAP1 target is located close to, but does not overlap, the target of the prior-art RNA polymerase inhibitor and antimycobacterial agent rifampin (Figure ; identities of residues of rifampin target as in [Ho, M., Hudson, B., Das, K., Arnold, E., Ebright, R. (2009) *Curr. Opin. Structl. Biol.* 19, 715-723]). Based on the absence of overlap between the AAP1 target and the rifampin target, we can infer that AAPs will not exhibit any cross-resistance with rifampicin and vice-versa.

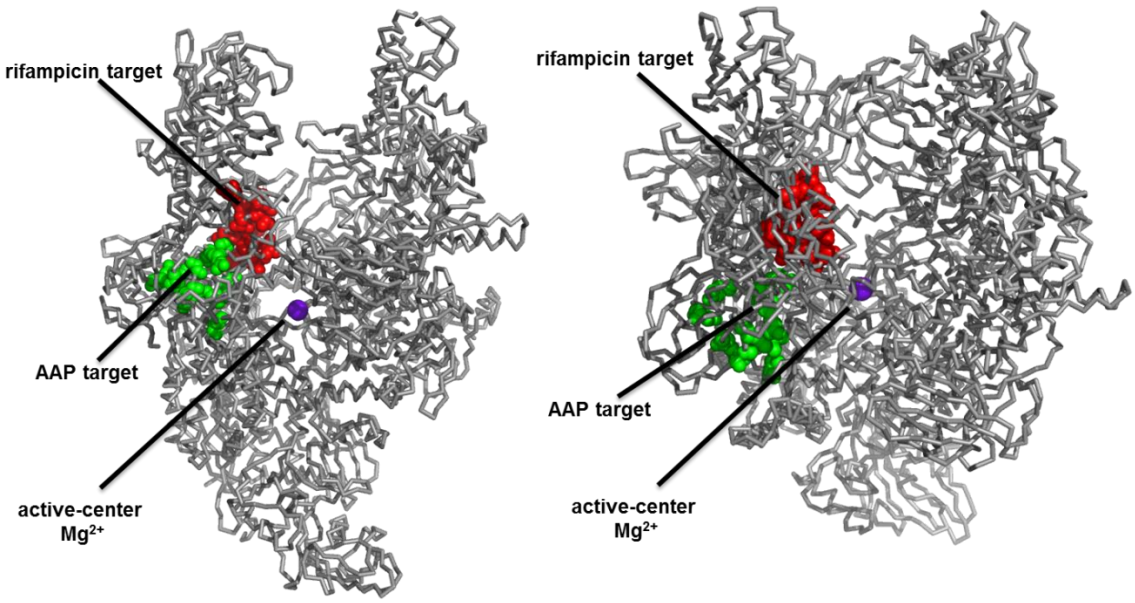

Figure 11: Location of AAP and rifampin target within bacterial RNAP.

In green are the amino-acid residues responsible for AAP-resistance, in red are amino-acid residue conferring rifampicin resistance, in purple Mg^{2+}. For clarity β' non-conserved region and σ subunit is removed. View as in Figure: 7

Thermus *thermophilus* RNAP holoenzyme at 3.3 Å resolution. Atomic coordinates taken from PDB accession code: 1IW7

4.2.7.2: Rifampicin cross-resistance level of AAP-resistant mutants: *Mycobacterium smegmatis*

To determine whether AAP resistant mutants exhibit cross-resistance to rifampicin, MICs of AAP1-resistant mutants for rifampicin were measured. One of the biggest threats in TB treatment is emergence of drug resistant-TB in which the TB bacilli become resistant

to (one of the primary line antibiotic) or multi-drug resistant TB (where the bacteria become resistant to more than one primary line antibiotic). Currently rifampicin is administered as one of the primary line antibiotic against TB and the rate of resistance against rifampicin is $1X10^{8}$. Rifampicin resistance arises due to mutation (point mutation, deletion, insertion) in the *rpoB* gene. In TB treatment to diminish the chance of emergence of drug-resistant TB combination therapy used, in which more than one antibiotic drug is prescribed at a given time, it is essential for the antibiotics to not exhibit cross-resistance. Hence, it is desirable that AAP target on RNAP does not overlap with rifampicin binding target and also, both the bacterial RNAP inhibitor does not exhibit cross-resistance.

To determine the level of Rifampicin cross-resistance, rifampicin MIC was determined for AAP1-resistant *M. smegmatis* mutant derivatives using broth dilution method. As a control experiment the MIC of wild-type *M*. *smegmatis* was determined and the MIC value was observed to be 3.125 µg/ml. The level of resistance was calculated as the ratio of observed MIC of AAP-resistant mutant over MIC of wild-type *M*. *smegmatis.*

Based on the result from the above experiments, none of the mutants were found to exhibit cross-resistance to rifampin (Table 13). In fact, some AAP1 resistant mutants were found to be hypersensitive to rifampin (Table 13).

Table 13: Level of rifampicin cross-resistance in AAP1-resistant mutant: *Mycobacterium smegmatis*

amino acid substitution	cross-resistance level ($MIC/MIC_{wild\text{-}type}$)
***rpoB* (RNAP β subunit)**	
468 pro→Ser	1
470 His→Arg	0.5
477 Ile→Phe	1
553 Arg→Cys	0.5
553 Arg→Gly	1
553 Arg→Pro	1
557 Gly→Ser	1
559 Val→Gly	1
571 Asp→Gly	0.5
576 Gln→Arg	0.5
***rpoC* (RNAP β' subunit)**	
833 Arg→Gly	1
850 Ile→Ser	0.5

4.2.7.2: AAP1 cross-resistance level of rifampicin-resistant mutants: *Mycobacterium smegmatis*

To confirm the fact that AAP1 and rifampicin does not exhibit cross-resistance reciprocal experiment was also performed in which AAP1 cross-resistance level was determined for isolated Rifampicin-resistant *M. smegmatis* mutants.

More than 70% of the rifampicin-resistant clinical isolates contain mutation at three locations in RNAP β-subunit *(E*. *coli* residue) 516 D, 526 H and 531 S [135] . We isolated two rifampicin-resistant mutant 442H→T (526) and 447S→L (531) in *M. smegmatis* (characterized by sequencing *rpoB* gene). AAP1 MIC was determined for the rifampin-resistant *M. smegmatis* mutants by broth dilution method. As a control experiment the AAP1 MIC value was determined for wild-type *M*. *smegmatis* the observed AAP1 MIC value for wild-type *M*. smegmatis was observed to be 0.39 µg/ml. The level of cross-resistance was calculated as the ratio of observed AAP1 MIC value of rifampicin-resistant mutant over the AAP1 MIC value for wild-type *M*. *smegmatis.*

Based on the result from the above experiment none of the rifampin-resistant mutants were found to exhibit cross-resistance to AAP1 (Table 14). In fact one of the rifampin-resistant mutants was observed to be hypersensitive to AAP1 (Table 14).

Table 14: Level of AAP-cross-resistance in rifampicin-resistant mutants: *Mycobacterium smegmatis*

amino acid substitution	**cross-resistance level ($MIC/MIC_{wild-type}$)**
***rpoB* (RNAP β subunit)**	
442 His→Tyr(=526 in *E*. *coli*)	1
447 Ser→leu(=531 in *E*. *coli*)	0.5

The observed absence of cross-resistance between rifampicin and AAP1, and the reciprocal absence of cross-resistance between rifampin and AAP1, are consistent with the absence of overlap between the AAP1 target and the rifampin target (Figure 11).

4.2.7.3: Rifampicin, myxopyronin, lipiarmycin cross-resistance level of AAP-resistant mutants: *Mycobacterium tuberculosis*:

To confirm the absence of cross-resistance between rifampicin and AAP1 in the causative agent of TB, we have determined the level of rifampicin cross-resistance in AAP-resistant *M*. *tuberculosis* mutants. Additionally we have also determined the cross-resistance level of two other RNAP inhibitors myxopyronin and lipiarmycin, they are both bacterial RNAP inhibitor with distinct binding target on bacterial RNAP than AAP1 or rifampicin. Myxopyronin binding target on bacterial RNAP is the switch region, and is distinct from Rifampicin and AAP1 binding target. lipiarmycin binding target is SWI/SW2 sub-region and it interferes with the RP_o formation. We performed MABA-MIC assays to test the level of cross-resistance between AAP-resistant *M. tuberculosis* H37Rv $mc^2$6230 and rifampicin, myxopyronin and lipiarmycin. As a control experiment the MIC value for each of the inhibitors against wild-type *M*. *tuberculosis* H37Rv $mc^2$6230 was determined and the level of cross-resistance was calculated based on the ratio of observed MIC value of mutant derivative over wild-type. The MIC values for the wild-type *M*. *tuberculosis* H37Rv $mc^2$6230 for rifampicin, lipiarmycin, myxopyronin were observed to be 0.012 µg/ml, 3.12 µg/ml, 25 µg/ml respectively. The results from the MABA-MIC assays indicate that none of the AAP-resistant mutant derivative exhibit cross-resistance to Tb drug rifampicin and other RNAP inhibitors, myxopyronin and lipiarmycin. In fact, one of the AAP-resistant mutants exhibited hypersensitivity to rifampicin. The result is consistent with the fact that the AAP-target does not overlap with binding target of rifampicin, lipiarmycin and myxopyronin (Table 15). The result is also consistent with the result from AAP-resistant mutant *M*. *smegmatis* derivative.

Table 15: Level of RNAP inhibitor-cross-resistance in AAP-resistant mutants: *M. tuberculosis*

amino acid substitution	cross-resistance level (MIC/MIC$_{wild\text{-}type}$)		
	rifampicin	myxopyronin	lipiarmycin
***rpoB* (RNAP β subunit)**			
473 Pro→Thr	1	1	1
558 Arg→Gly	0.5	1	1
558 Arg→Ser	1	1	1
581 Gln→Arg	0.12	1	1

5. Mechanism of inhibition: AAPs

Since AAP target on RNAP does not overlap with the active center, we determined the mechanism of inhibition of AAPs. We assessed the effect of AAPs on different step of transcription (initiation and elongation).

In an identical experiment we compared the effect of AAPs and Rifampicin on the mechanism of transcription inhibition

Also, since AAP and CBR703 target are identical we examined the effect of CBR703 on *M*. *tuberculosis* RNAP and vice versa.

5.1 Materials and methods:

5.1.1 *De-novo* transcription initiation assay: radiochemical in-vitro transcription assay

Reaction mixtures (9.3 µl) contained: 40 nM *M. tuberculosis* RNAP core and σ^A (incubated on ice for 10 minutes to form holoenzyme), 10 nM N25, 10 µM, 40 µM of AAP1 and AAP12 respectively and 0.2 µM rifampicin, 40 mM Tris (pH 8.0), 75 mM NaCl, 5 mM $MgCl_2$, 2.5 mM DTT,12.5 % glycerol Reaction components other than DNA were incubated for 10 min at 37 °C prior to addition of DNA. Following 10 min at 37 °C, 0.5 µl 2 mM ATP and 0.2 µl [α-32P]UTP 40mCi/ml were added, and, following a further 10 min at 37 °C, reaction mixtures were supplemented with 5 µl loading buffer (10 mM EDTA, 0.02% bromophenol blue, 0.02% xylene cyanol, and 80% formamide), and boiled for 3 min at 95 ℃. Samples were applied to 24% polyacrylamide gels (19:1

acrylamide:bisacrylamide), electrophoresed in 90 mM Tris-borate (pH 8.0) and 2 mM EDTA, and analysed by storage-phosphor scanning (Typhoon; GE Healthcare, Inc.).

5.1.2 Primer-dependent transcription initiation assay: radiochemical *in-vitro* transcription assay.

Reaction mixtures (8.1 ml) contained 40 nM *M. tuberculosis.* RNAP core and 120 nM σA (incubated on ice for 10 mines to form holoenzyme), either none or one of antibiotics (10 mM and 40 µM of AAP1 and AAP12 respectively, 0.2 mM rifampicin, 40 mM CBR703), 40 mM Tris (pH 8.0), 75 mM NaCl, 5 mM $MgCl_2$, 2.5 mM DTT,12.5 % glycerol. Reaction mixtures were incubated at 37 °C for 10 minutes, supplemented with 0.5 ml 0.2 mM LacUV5-ICAP DNA, and incubated at 37 °C for 10 minutes. Reactions were initiated with 0.9 ml NTP subset (125 mM UTP, 0.1 µl of [α-32P]UTP 40mCi/ml, 5.6 mM ribodinucleotide ApA), and allowed at 37 °C for 10 minutes. Reactions mixtures were subsequently supplemented with 10 µl loading buffer (10 mM EDTA, 0.02% bromophenol blue, 0.02% xylene cyanol, and 80% formamide), and boiled for 4 min at 95 °C Samples were applied to 15% polyacrylamide gels (19:1 acrylamide:bisacrylamide), electrophoresed in 90 mM Tris-borate (pH 8.0) and 2 mM EDTA, and analyzed by storage-phosphor scanning (Typhoon; GE Healthcare, Inc.).

5.1.3 Transcription elongation: radiochemical in-vitro transcription assay

Reactions mixture (10.5 ml) contained 40 nM *M. tuberculosis.* RNAP core and 120 nM σ^A (incubated in ice for 10 minutes to form holoenzyme), 10 nM N25-100-tR2 DNA template, 40 mM Tris (pH 8.0), 75 mM NaCl, 5 mM $MgCl_2$, 2.5 mM DTT,12.5 % glycerol. Reaction mixtures were incubated at 37 °C for 10 minutes Reactions were initiated with 2.2 µl NTP subset without CTP (34 mM GTP, 34 mM UTP, 34 mM ATP and 0.2 µl [α-32P]UTP 40mCi/ml, and allowed at 37 °C for 2.5 minutes. The transcription reaction

was expected to halt at G29 position. The reaction mixtures were then incubated with 0.75 ml DMSO or one of inhibitors (10 µM and 40 µM of AAP1 and AAP12 respectively, and 0.2 µM of rifampicin) for 5 minutes at 37 °C. The reactions were restarted with 0.75 ml 100 mM CTP, and allowed at 37 °C for 2.5 min. Reactions mixtures were subsequently supplemented with 10 µl loading buffer (10 mM EDTA, 0.02% bromophenol blue, 0.02% xylene cyanol, and 80% formamide), and boiled for 4 min at 95 ℃. Samples were applied to 15% polyacrylamide gels (19:1 acrylamide:bisacrylamide), electrophoresed in 90 mM Tris-borate (pH 8.0) and 2 mM EDTA, and analyzed by storage-phosphor scanning (Typhoon; GE Healthcare, Inc.).

5.2 Results and conclusion: Mechanism of AAPs inhibition:

To determine the effect of AAPs on transcription initiation, we have performed 1) *de-novo* initiation and 2) primer dependent transcription initiation assays.

5.2.1 Effect of AAPs on transcription: *de-novo* initiation:

To assess the effect of AAPs on de-novo transcription initiation, we have performed radiochemical transcription assay. We used N25 promoter DNA (Figure 12), and examined the formation of ApU (dinucleotide product) by using ATP and radioactive [α-32P]-UTP. The dinucleotide product ApU* was electrophoresed and resolved on a 24% denaturing sequencing gel. We examined the effect of AAPs (AAP1 and AAP12) and rifampicin (inhibits transcription by sterically blocking formation of RNA product more than 2 or 3 nt) in the transcription elongation experiment

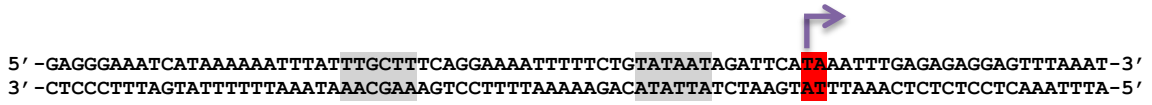

Figure 12: N25 promoter DNA

Part of the N25 promoter DNA. The start site (ApU RNA product) is in red and the upstream -10 and -35 regions are shaded.

We observed that AAP1 and AAP12 inhibits the formation of ApU dinucleotide (Figure 14A) at concentration 10 µM and 40 µM, whereas in the same experiment rifampicin at concentration 0.2 µM does not inhibit the formation of ApU.

5.2.2 Effect of AAPs on primer-dependent transcription initiation

To determine the effect of AAPs on primer dependent transcription initiation, we performed a radiochemical transcription assay. For this experiment we used lacUV5 promoter DNA (Figure 13) and ApA primer, which upon addition of UTP forms two products trinucleotide (ApApU) and tetranucleotide (ApApUpU). In this experiment the enzyme was first incubated with inhibitors, followed by addition of promoter DNA and finally transcription reaction was initiated by addition of ApA primer and UTP. We resolved the trinucleotide and tetranucleotide product on a 15% sequencing denaturing gel. We examined the effect of both AAPs and rifampicin on primer dependent transcription initiation. Rifampicin in the same experiment is known to inhibit the

formation of tetranucleotide transcription initiation transcription product but does not affect formation of trinucleotude product.

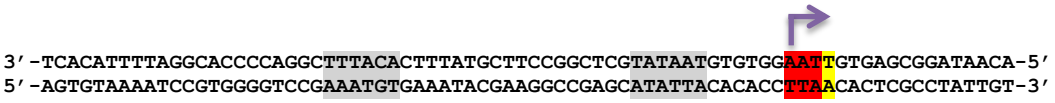

Figure 13: LacUV5 promoter DNA

Fragment of promoter DNA. The start site (ApA RNA product) is in red and the upstream -10 and -35 regions are shaded.

We observed that both AAP1 and AAP12 inhibit the formation of both trinuleotide and tetranuleotide products at concentration of 10 µM and 40 µM each, in the identical experiment rifamipcin at concentration 0.2 µM inhibits the formation of tetranucleotide but not the trinucleotide.

The results indicate that AAPs can inhibit transcription initiation by *Mycobacterium tuberculosis* RNAP in both *de novo* and primer extension reaction. The result also indicates that AAPs and rifampicin mode of transcription inhibition is not identical. Based on these observations we can propose that AAPs are inhibitors of *Mycobacterium tuberculosis* RNAP inhibiting transcription at the stage of initiation and the mechanism of transcription initiation inhibition by AAPs and the TB drug rifampicin differs from each other

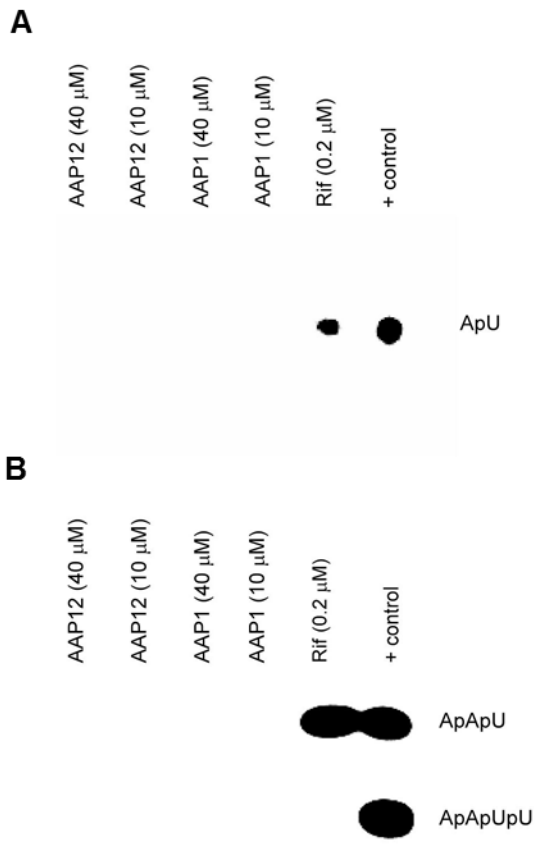

Figure 14: Effect of AAPs on transcription initiation: Mycobacterium *tuberculosis* RNAP

A) *de-novo* synthesis assay
Product resolved on 24% denaturing sequencing PAGE
In de-novo synthesis assay no inhibitor lane contains + control and shows the dinucleotide product.
AAP1 and AAP12 contains inhibitors at 10 and 40 µM and exhibit inhibition of formation of dinucleotide product whereas rifampicin at 0.2 µM does not inhibit the formation of dinucleotide product

B) Primer-dependent initiation assay
Product resolved on 15% denaturing sequencing PAGE
+ control contains no inhibitor and shows the formation of trinucleotide and tetranuceotide products.
AAP1 and AAP12 at concentration of 10 and 40 µM inhibit the formation of any transcription product.
Rifampicin at 0.2 µM in the experiment inhibits the formation of tetranucleotide but not trinucleotide product.

5.2.3 Effect of AAPs on transcription elongation

After determining the effect of AAPs on transcription initiation we probed the effect of these inhibitors on the next step of transcription which is elongation. To do so we have performed a radiochemical transcription assay and in the assay we used N25 tr-100 promoter DNA (Figure 15), which forms a 29 nt (G29) halt product when CTP is not included in the transcription reaction. In the reaction we added enzyme, promoter DNA and all NTPs without CTP, after incubating the reaction for appropriate time inhibitors were added, after incubation with the Inhibitors we resumed the transcription reaction by addition of CTP to form the full length 100 nucleotide run-off transcript. We resolved the G29 product from the run-off 100 nt product by electrophoresing the transcription reaction on a 15% denaturing sequencing gel. We examined the effect of AAP1, AAP12 and rifampicin on transcription elongation and compared the observed result of each inhibitor. Rifampicin is known to sterically block the formation of nascent RNA formation of 2-3 nucleotide and does not affect RNAP after it enters elongation complex, hence in this experiment we do not expect to observe any inhibitory effect from rifampicin.

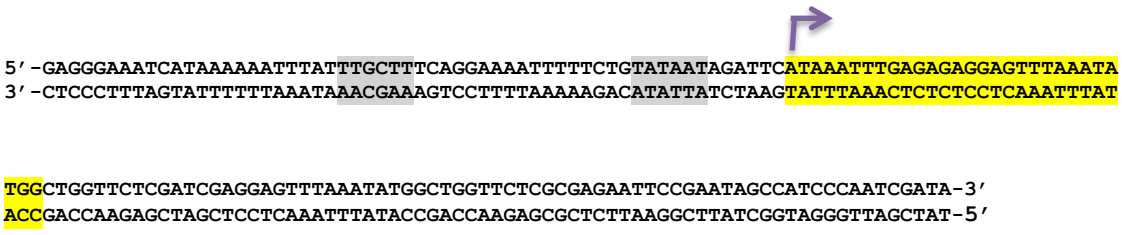

Figure 15: N25-tr2-100 promoter DNA

The G29 nucleotide transcript is in yellow, upstream promoter binding region -35 and -10 are shaded in shaded in gray.

In the above reaction we observed that both AAP1 and AAP12 at concentration 40 µM inhibited the elongation of G29 nucleotide. Rifampicin in the same experiment did not have any effect on transcription elongation (as expected based on the known mechanism) (Figure 16). Based on this observation we can infer that AAPs can inhibit transcription by *Mycobacterium tuberculosis* RNAP in transcription elongation reaction and that the mechanistic effect of AAP differs from that of rifampicin. Hence we propose that AAPs are inhibitors of *Mycobacterium tuberculosis* RNAP and can inhibit transcription at the stage of elongation and the mechanism of inhibition varies from that of the TB drug rifampicin. Since, AAPs can inhibit both transcription initiation and elongation and the effect of AAPs is analogous with the effect of CBR703 on *E*. *coli* RNAP, and also based on the fact that the binding target of CBR703 and AAPs are identical, we can propose that AAPs inhibits mycobacterial RNAP with identical mechanism as CBR703 inhibits *E*. *coli* RNAP [106]. The mechanism of transcription inhibition of CBR703 is determined and it is proposed that CBR703 interfere with the RNAP nucleotide addition cycle. Thus, we can propose that AAPs inhibits or interferes with the nucleotide addition cycle of *Mycobacterium tuberculosis* RNAP and hence, inhibits transcription at both initiation and elongation stage. Also, the mechanism of transcription inhibition by AAPs is different than the known RNAP inhibitor rifampicin and this observation is consistent with the fact that the binding target of AAPs and rifampicin does not overlap and also consistent with the fact that AAPs and rifampicin does not exhibit any cross-resistance.

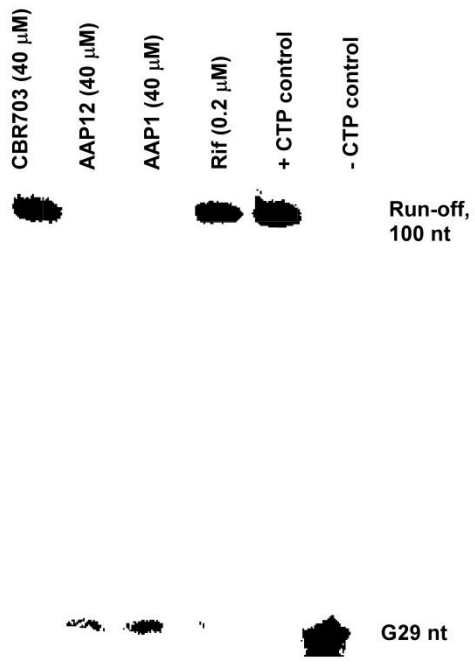

Figure 16: Effect of AAPs on transcription elongation: Mycobacterium *tuberculosis* RNAP

Product resolved on 15% denaturing sequencing PAGE

- CTP Control contains no CTP and no inhibitors in the reaction mixture and shows G29 product

+CTP contains no inhibitors and shows the 100 nt full-length run-off transcript

+Rif contains rifampicin at 0.2 μM concentration and shows no inhibition of elongation from G29 to 100 nt

AAP1 and AAP12 at concentration of 40 μM inhibits the formation of elongation of G29 product

CBR703 at 40μM concentration does not inhibit the formation of elongation product.

Discussion:

Tuberculosis despite being an ancient disease still remains the second largest cause of mortality from infection. Resurgence of TB epidemic has emerged due to HIV infection and persistence of drug-resistance TB. The disease was declared a global health emergency in 1993, and requires urgent attention in terms of its treatment and cure. In 2006 a high-throughput screening was performed to identify compounds with antimycobacterial characteristics. Out of 114,260 compounds screened five compounds were identified as top hit. Out of the five compounds two of them had the same scaffold of AAPs and AAP1.

In this work we demonstrate the functional cellular target of AAPs as bacterial RNAP, and also identify the binding target of AAPs within the bacterial RNAP.

AAPs stereo-selectively inhibit Mycobacteria:

In the current study we have determined the species specificity and stereo-specificity of a compound isolated through high-throughput screening against mycobacterial RNAP. We have assessed the effect of AAPs in *in-vitro* transcription assays performed against purified *M. tuberculosis, E. coli* and *S. aureus* RNAP. The result indicates that AAPs exhibit potent activity against only mycobacterial RNAP and that AAPs exhibit poor or no activity against RNAP from other non-bacterial species. We determined the antibacterial activity of AAPs against *M. tuberculosis*, *M. smegmatis, E. coli, S. aureus* and various other fast-growing thermophilic mycobacteria and observed that AAPs exhibits the same trend as observed in *in-vitro* transcription assays. Based on the results from these

assays we propose that AAPs are species specific inhibitor of mycobacteria (with enhanced potency).

Since, AAPs possesses a chiral center, we determined the stereo-specific activity of AAP1 by assessing the effect of D-AAP1, L-AAP1 and D/L-AAP1 on the inhibition of mycobacterial RNAP and on inhibition of mycobacterial growth. Based on the result, we observed that D-AAP1 was >100 fold more active than L-AAP1.in transcription assay, this trend was also observed in mycobacterial growth inhibition assay where D-AAP1 exhibited >100 fold activity (*Mycobacterium smegmatis*). Hence, we propose that the antimycobacterial action of AAP1 is stereoisomer specific and that "D-AAP1" is the isomer responsible for exhibiting antimycobacterial activity.

AAP target and property:

We have determined and identified the functional cellular target of AAPs as the bacterial RNAP by the isolation of spontaneous resistant mutants. We have also determined the binding target of AAPs on bacterial RNAP by mapping the amino acid residues responsible for conferring AAP resistance on the three-dimensional structure of bacterial RNAP. We determined that the target of AAP within bacterial RNAP is a site, adjacent to the active center, but not overlapping with the active center residues. This proposed AAP binding target does not overlap with RNAP's nucleic acid binding determinant, sigma binding determinant or the catalytic center and is located at the base of β-lobe and the N-terminal of β' bridge helix. This binding site of AAPs in mycobacterial RNAP is essentially identical to the binding site of CBR703 (Gram-negative ligand specific inhibitor) on E. *coli* RNAP.

Our results show that the AAP binding target is located adjacent to the rifampicin binding target but does not overlap. This is consistent with the fact that the AAP-

resistant mutant does not exhibit any cross-resistance to the current TB drug rifampicin and vice versa. We have also determined the rate of resistance for AAP in mycobacteria and observed that the rate of mutation is similar to that of rifampicin.

AAPs mechanism of inhibition:

We have probed AAPs' mechanism of mycobacterial RNAP inhibition and determined that AAPs inhibits transcription at stage of initiation (*de novo* and primer dependent) and elongation. We have shown that AAPs' mechanism of mycobacterial RNAP inhibition differs from that of rifampicin's mechanism of RNAP inhibition (consistent with the difference in binding site). We have also established that CBR703 an *E*. *coli* RNAP specific inhibitor with identical target as AAPs does not inhibit mycobacterium RNAP in the transcription initiation assay and vice-versa but their mechanism of inhibition is identical for their respective target [106].

Based on the location of AAPs' target within bacterial RNAP and the mechanism of inhibition we propose that AAPs are allosteric inhibitor of mycobacterial RNAP. Since, bridge helix is known to participate in nucleotide addition cycle and undergoes conformation change during the nucleotide addition cycle. We propose that AAPs function by interfering with the bridge helix conformational dynamics and hence affecting the nucleotide addition cycle. Possibly, AAPs hold the bridge helix in a straight conformation by binding at the bridge helix N-terminal subsite (mechanism identical to CBR703).

Introduction of rifampicin in the course of TB treatment has proven to be a breakthrough in terms of reduction in the length of treatment and sterilizing effect on the persisters. In the current scenario, emergence of rifampicin-resistant TB has threatened the clinical utility of rifamycin class of compounds. Also, due to rifampicin's limitations in

the treatment of in HIV-TB and scarcity of sterilizing drugs in TB treatment demands for the urgent need to explore new RNAP inhibitor [124].

In this study we introduce a new class of mycobacterial RNAP inhibitors, which act on mycobacterial RNAP at a different target than rifampicin, functions through a different mechanism than rifampicin and also exhibit similar or less susceptibility to grow resistant mutants than rifampicin. In collaborative work with Dr. Nancy Connell and Dr. Meliza Talaue at Rutgers Newark we have observed that AAPs exhibit potent sterilizing activity against non-replicative mycobacteria) and on rifampicin-resistant non-replicative mycobacteria (Hu coates model III). Also, in the collaborative work with Dr. Janasy Sarathy and Dr. Veronique Dartois at Rutgers Newark we have observed that AAPs exhibit greater intracellular accumulation in rifampicin-resistant non-replicating mycobacteria, which accounts for the enhanced sterilizing effect of AAPs.

AAPs have potential drug like properties, which is it does not exhibit any liability in *in-vitro* ADME studies and also excellent result in preliminary pharmacokinetic study (enhanced half-life in rat PK iv and oral)

All these properties, together with the fact that AAPs are bacterial RNAP-specific inhibitors (do not affect eukaryotic RNAP in transcription assays and do not inhibit eukaryotic cell growth), make AAPs promising candidates for developing AAPs as drugs in TB treatment or in treating mycobacterial infection.

In future, introduction of another RNAP inhibitor (besides rifampicin) that can be co-administered with rifampicin for the treatment of TB, could enhance the sterilizing effect on the persisters leading to overall enhancement of potency and ultimately decreasing the treatment duration. Also, AAPs' and rifampicin co-administration could diminish the chance of emergence of spontaneous resistant-mutants to either drugs and

at the same time exhibit additive or superadditive effects on *Mycobacterium tuberculosis* growth inhibition. Additionally, since AAPs exhibit sterilizing activity against rifampicin-resistant *Mycobacterium tuberculosis* it could be used as a drug in treating MDR-TB and XDR-TB, which is highly desirable.

Since, AAPs have modular structure (consist of three rings A, B and C) and can be synthesized in a single step reaction, lead optimization using the single substitution walk method can be performed in the three rings (A, B and C) in facile manner. In our current work using the approach of “systematic lead optimization”, we have tested more than 400 AAP1 analogs, and successfully identified compounds with >8 fold higher potency against *Mycobacterium tuberculosis* in *in-vitro* transcription assays and growth inhibition assays. The goal is to combine the desirable property of each substitution to achieve greater potency and efficacy. Additionally, we are focusing on improving the physical and pharmacological properties of AAPs, and also identifying compounds suitable for evaluation in animal models of tuberculosis.

In current study we are also performing experiments to determine the effect of the synthesized analogs of AAPs against RNAP from *E. coli* and *S. aureus* to identify a ligand that can inhibit either Gram-negative, Gram-positive or both bacterial species. The idea is to identify and develop broad-spectrum bacterial inhibitor thereby increasing the scope of activity and utility of AAPs.

Reference:

1. Sweetser, D., M. Nonet, and R.A. Young, *Prokaryotic and eukaryotic RNA polymerases have homologous core subunits.* Proc Natl Acad Sci U S A, 1987. **84**(5): p. 1192-6.

2. Ebright, R.H., *RNA polymerase: structural similarities between bacterial RNA polymerase and eukaryotic RNA polymerase II.* J Mol Biol, 2000. **304**(5): p. 687-98.

3. Darst, S.A., *Bacterial RNA polymerase.* Curr Opin Struct Biol, 2001. **11**(2): p. 155-62.

4. Cramer, P., *Multisubunit RNA polymerases.* Curr Opin Struct Biol, 2002. **12**(1): p. 89-97.

5. Chopra, I., *Bacterial RNA polymerase: a promising target for the discovery of new antimicrobial agents.* Current opinion in investigational drugs, 2007. **8**(8): p. 600-7.

6. Villain-Guillot, P., et al., *Progress in targeting bacterial transcription.* Drug discovery today, 2007. **12**(5-6): p. 200-8.

7. Zhang, G., et al., *Crystal structure of Thermus aquaticus core RNA polymerase at 3.3 A resolution.* Cell, 1999. **98**(6): p. 811-24.

8. Murakami, K.S., S. Masuda, and S.A. Darst, *Crystallographic analysis of Thermus aquaticus RNA polymerase holoenzyme and a holoenzyme/promoter DNA complex.* Methods Enzymol, 2003. **370**: p. 42-53.

9. Vassylyeva, M.N., et al., *Purification, crystallization and initial crystallographic analysis of RNA polymerase holoenzyme from Thermus thermophilus.* Acta crystallographica. Section D, Biological crystallography, 2002. **58**(Pt 9): p. 1497-500.

10. Murakami, K.S., *X-ray crystal structure of Escherichia coli RNA polymerase sigma70 holoenzyme.* J Biol Chem, 2013. **288**(13): p. 9126-34.

11. Bae, B., et al., *Phage T7 Gp2 inhibition of Escherichia coli RNA polymerase involves misappropriation of sigma70 domain 1.1.* Proc Natl Acad Sci U S A, 2013. **110**(49): p. 19772-7.

12. Campbell, E.A., et al., *Structural mechanism for rifampicin inhibition of bacterial rna polymerase.* Cell, 2001. **104**(6): p. 901-12.

13. Campbell, E.A., et al., *Structural, functional, and genetic analysis of sorangicin inhibition of bacterial RNA polymerase.* EMBO J, 2005. **24**(4): p. 674-82.

14. Mukhopadhyay, J., et al., *The RNA polymerase "switch region" is a target for inhibitors.* Cell, 2008. **135**(2): p. 295-307.

15. Ho, M.X., et al., *Structures of RNA polymerase-antibiotic complexes.* Curr Opin Struct Biol, 2009. **19**(6): p. 715-23.

16. Ebright, R.H. and S. Busby, *The Escherichia coli RNA polymerase alpha subunit: structure and function.* Curr Opin Genet Dev, 1995. **5**(2): p. 197-203.

17. Ishihama, A., *Subunit of assembly of Escherichia coli RNA polymerase.* Advances in biophysics, 1981. **14**: p. 1-35.

18. Burgess, R.R., et al., *Factor stimulating transcription by RNA polymerase.* Nature, 1969. **221**(5175): p. 43-6.

19. Korzheva, N., et al., *A structural model of transcription elongation.* Science, 2000. **289**(5479): p. 619-25.

20. Naryshkin, N., et al., *Structural organization of the RNA polymerase-promoter open complex.* Cell, 2000. **101**(6): p. 601-11.

21. Dieci, G., et al., *A universally conserved region of the largest subunit participates in the active site of RNA polymerase III.* EMBO J, 1995. **14**(15): p. 3766-76.

22. Martinez-Rucobo, F.W. and P. Cramer, *Structural basis of transcription elongation.* Biochimica et biophysica acta, 2013. **1829**(1): p. 9-19.

23. Cramer, P., D.A. Bushnell, and R.D. Kornberg, *Structural basis of transcription: RNA polymerase II at 2.8 angstrom resolution.* Science, 2001. **292**(5523): p. 1863-76.

24. Cramer, P., et al., *Architecture of RNA polymerase II and implications for the transcription mechanism.* Science, 2000. **288**(5466): p. 640-9.

25. Nickels, B.E. and A. Hochschild, *Regulation of RNA polymerase through the secondary channel.* Cell, 2004. **118**(3): p. 281-4.

26. Kettenberger, H., K.J. Armache, and P. Cramer, *Complete RNA polymerase II elongation complex structure and its interactions with NTP and TFIIS.* Mol Cell, 2004. **16**(6): p. 955-65.

27. Vassylyev, D.G., et al., *Structural basis for substrate loading in bacterial RNA polymerase.* Nature, 2007. **448**(7150): p. 163-8.

28. Westover, K.D., D.A. Bushnell, and R.D. Kornberg, *Structural basis of transcription: nucleotide selection by rotation in the RNA polymerase II active center.* Cell, 2004. **119**(4): p. 481-9.

29. Chakraborty, A., et al., *Opening and closing of the bacterial RNA polymerase clamp.* Science, 2012. **337**(6094): p. 591-5.

30. Gnatt, A.L., et al., *Structural basis of transcription: an RNA polymerase II elongation complex at 3.3 A resolution.* Science, 2001. **292**(5523): p. 1876-82.

31. Lara-Gonzalez, S., J.J. Birktoft, and C.L. Lawson, *Structure of the Escherichia coli RNA polymerase alpha subunit C-terminal domain.* Acta crystallographica. Section D, Biological crystallography, 2010. **66**(Pt 7): p. 806-12.

32. Vassylyev, D.G., et al., *Crystal structure of a bacterial RNA polymerase holoenzyme at 2.6 angstrom resolution.* Nature, 2002. **417**(6890): p. 712-719.

33. Lawson, C.L., et al., *Catabolite activator protein: DNA binding and transcription activation.* Curr Opin Struct Biol, 2004. **14**(1): p. 10-20.

34. Mathew, R. and D. Chatterji, *The evolving story of the omega subunit of bacterial RNA polymerase.* Trends in microbiology, 2006. **14**(10): p. 450-5.

35. Minakhin, L., et al., *Bacterial RNA polymerase subunit omega and eukaryotic RNA polymerase subunit RPB6 are sequence, structural, and functional homologs and promote RNA polymerase assembly.* Proc Natl Acad Sci U S A, 2001. **98**(3): p. 892-7.

36. Murakami, K.S. and S.A. Darst, *Bacterial RNA polymerases: the wholo story.* Curr Opin Struct Biol, 2003. **13**(1): p. 31-9.

37. Gross, C.A., et al., *The functional and regulatory roles of sigma factors in transcription.* Cold Spring Harb Symp Quant Biol, 1998. **63**: p. 141-55.

38. Mooney, R.A., S.A. Darst, and R. Landick, *Sigma and RNA polymerase: an on-again, off-again relationship?* Mol Cell, 2005. **20**(3): p. 335-45.

39. Gruber, T.M. and D.A. Bryant, *Molecular systematic studies of eubacteria, using sigma70-type sigma factors of group 1 and group 2.* J Bacteriol, 1997. **179**(5): p. 1734-47.

40. Lonetto, M., M. Gribskov, and C.A. Gross, *The sigma 70 family: sequence conservation and evolutionary relationships.* J Bacteriol, 1992. **174**(12): p. 3843-9.

41. Murakami, K.S., S. Masuda, and S.A. Darst, *Structural basis of transcription initiation: RNA polymerase holoenzyme at 4 A resolution.* Science, 2002. **296**(5571): p. 1280-4.

42. Murakami, K.S., et al., *Structural basis of transcription initiation: an RNA polymerase holoenzyme-DNA complex.* Science, 2002. **296**(5571): p. 1285-90.

43. Campbell, E.A., et al., *Structure of the bacterial RNA polymerase promoter specificity sigma subunit.* Mol Cell, 2002. **9**(3): p. 527-39.

44. Dombroski, A.J., W.A. Walter, and C.A. Gross, *Amino-terminal amino acids modulate sigma-factor DNA-binding activity.* Genes Dev, 1993. **7**(12A): p. 2446-55.

45. Camarero, J.A., et al., *Autoregulation of a bacterial sigma factor explored by using segmental isotopic labeling and NMR.* Proc Natl Acad Sci U S A, 2002. **99**(13): p. 8536-41.

46. Mekler, V., et al., *Structural organization of bacterial RNA polymerase holoenzyme and the RNA polymerase-promoter open complex.* Cell, 2002. **108**(5): p. 599-614.

47. Marr, M.T. and J.W. Roberts, *Promoter recognition as measured by binding of polymerase to nontemplate strand oligonucleotide.* Science, 1997. **276**(5316): p. 1258-60.

48. Zhang, Y., et al., *Structural basis of transcription initiation.* Science, 2012. **338**(6110): p. 1076-80.

49. Ross, W., et al., *A third recognition element in bacterial promoters: DNA binding by the alpha subunit of RNA polymerase.* Science, 1993. **262**(5138): p. 1407-13.

50. Lisser, S. and H. Margalit, *Compilation of E. coli mRNA promoter sequences.* Nucleic Acids Res, 1993. **21**(7): p. 1507-16.

51. deHaseth, P.L. and J.D. Helmann, *Open complex formation by Escherichia coli RNA polymerase: the mechanism of polymerase-induced strand separation of double helical DNA.* Mol Microbiol, 1995. **16**(5): p. 817-24.

52. Haugen, S.P., et al., *rRNA promoter regulation by nonoptimal binding of sigma region 1.2: an additional recognition element for RNA polymerase.* Cell, 2006. **125**(6): p. 1069-82.

53. Feklistov, A., et al., *A basal promoter element recognized by free RNA polymerase sigma subunit determines promoter recognition by RNA polymerase holoenzyme.* Mol Cell, 2006. **23**(1): p. 97-107.

54. Ponnambalam, S., et al., *Transcription initiation at the Escherichia coli galactose operon promoters in the absence of the normal -35 region sequences.* J Biol Chem, 1986. **261**(34): p. 16043-8.

55. Saecker, R.M., M.T. Record, Jr., and P.L. Dehaseth, *Mechanism of bacterial transcription initiation: RNA polymerase - promoter binding, isomerization to initiation-competent open complexes, and initiation of RNA synthesis.* J Mol Biol, 2011. **412**(5): p. 754-71.

56. Lee, D.J., S.D. Minchin, and S.J. Busby, *Activating transcription in bacteria.* Annual review of microbiology, 2012. **66**: p. 125-52.

57. Komissarova, N. and M. Kashlev, *Functional topography of nascent RNA in elongation intermediates of RNA polymerase.* Proc Natl Acad Sci U S A, 1998. **95**(25): p. 14699-704.

58. Steitz, T.A., *A mechanism for all polymerases.* Nature, 1998. **391**(6664): p. 231-2.

59. Revyakin, A., et al., *Abortive initiation and productive initiation by RNA polymerase involve DNA scrunching.* Science, 2006. **314**(5802): p. 1139-43.

60. Straney, S.B. and D.M. Crothers, *Kinetics of the stages of transcription initiation at the Escherichia coli lac UV5 promoter.* Biochemistry, 1987. **26**(16): p. 5063-70.

61. Hsu, L.M., *Promoter clearance and escape in prokaryotes.* Biochimica et biophysica acta, 2002. **1577**(2): p. 191-207.

62. Borukhov, S. and E. Nudler, *RNA polymerase: the vehicle of transcription.* Trends in microbiology, 2008. **16**(3): p. 126-34.

63. Kireeva, M.L., et al., *The 8-nucleotide-long RNA:DNA hybrid is a primary stability determinant of the RNA polymerase II elongation complex.* J Biol Chem, 2000. **275**(9): p. 6530-6.

64. Mukhopadhyay, J., et al., *Translocation of sigma(70) with RNA polymerase during transcription: fluorescence resonance energy transfer assay for movement relative to DNA.* Cell, 2001. **106**(4): p. 453-63.

65. Vassylyev, D.G., et al., *Structural basis for transcription elongation by bacterial RNA polymerase.* Nature, 2007. **448**(7150): p. 157-62.

66. Wang, D., et al., *Structural basis of transcription: role of the trigger loop in substrate specificity and catalysis.* Cell, 2006. **127**(5): p. 941-54.

67. Cheung, A.C., S. Sainsbury, and P. Cramer, *Structural basis of initial RNA polymerase II transcription.* EMBO J, 2011. **30**(23): p. 4755-63.

68. Zhang, J., M. Palangat, and R. Landick, *Role of the RNA polymerase trigger loop in catalysis and pausing.* Nat Struct Mol Biol, 2010. **17**(1): p. 99-104.

69. Sosunov, V., et al., *Unified two-metal mechanism of RNA synthesis and degradation by RNA polymerase.* EMBO J, 2003. **22**(9): p. 2234-44.

70. Steitz, T.A., *DNA and RNA polymerases: structural diversity and common mechanisms.* Harvey lectures, 1997. **93**: p. 75-93.

71. Feig, M. and Z.F. Burton, *RNA polymerase II with open and closed trigger loops: active site dynamics and nucleic acid translocation.* Biophys J, 2010. **99**(8): p. 2577-86.

72. Epshtein, V., et al., *Swing-gate model of nucleotide entry into the RNA polymerase active center.* Mol Cell, 2002. **10**(3): p. 623-34.

73. Bar-Nahum, G., et al., *A ratchet mechanism of transcription elongation and its control.* Cell, 2005. **120**(2): p. 183-93.

74. Tuske, S., et al., *Inhibition of bacterial RNA polymerase by streptolydigin: stabilization of a straight-bridge-helix active-center conformation.* Cell, 2005. **122**(4): p. 541-52.

75. Nudler, E., *RNA polymerase active center: the molecular engine of transcription.* Annual review of biochemistry, 2009. **78**: p. 335-61.

76. Brueckner, F., J. Ortiz, and P. Cramer, *A movie of the RNA polymerase nucleotide addition cycle.* Curr Opin Struct Biol, 2009. **19**(3): p. 294-9.

77. Abbondanzieri, E.A., et al., *Direct observation of base-pair stepping by RNA polymerase.* Nature, 2005. **438**(7067): p. 460-5.

78. Kireeva, M., M. Kashlev, and Z.F. Burton, *Translocation by multi-subunit RNA polymerases.* Biochimica et biophysica acta, 2010. **1799**(5-6): p. 389-401.

79. Borukhov, S., V. Sagitov, and A. Goldfarb, *Transcript cleavage factors from E. coli.* Cell, 1993. **72**(3): p. 459-66.

80. Zenkin, N., Y. Yuzenkova, and K. Severinov, *Transcript-assisted transcriptional proofreading.* Science, 2006. **313**(5786): p. 518-20.

81. Landick, R., *The regulatory roles and mechanism of transcriptional pausing.* Biochemical Society transactions, 2006. **34**(Pt 6): p. 1062-6.

82. Sydow, J.F. and P. Cramer, *RNA polymerase fidelity and transcriptional proofreading.* Curr Opin Struct Biol, 2009. **19**(6): p. 732-9.

83. Nudler, E., et al., *The RNA-DNA hybrid maintains the register of transcription by preventing backtracking of RNA polymerase.* Cell, 1997. **89**(1): p. 33-41.

84. Komissarova, N. and M. Kashlev, *Transcriptional arrest: Escherichia coli RNA polymerase translocates backward, leaving the 3' end of the RNA intact and extruded.* Proc Natl Acad Sci U S A, 1997. **94**(5): p. 1755-60.

85. Brueckner, F. and P. Cramer, *Structural basis of transcription inhibition by alpha-amanitin and implications for RNA polymerase II translocation.* Nat Struct Mol Biol, 2008. **15**(8): p. 811-8.

86. Kaplan, C.D., K.M. Larsson, and R.D. Kornberg, *The RNA polymerase II trigger loop functions in substrate selection and is directly targeted by alpha-amanitin.* Mol Cell, 2008. **30**(5): p. 547-56.

87. Bushnell, D.A., P. Cramer, and R.D. Kornberg, *Structural basis of transcription: alpha-amanitin-RNA polymerase II cocrystal at 2.8 A resolution.* Proc Natl Acad Sci U S A, 2002. **99**(3): p. 1218-22.

88. Wehrli, W. and M. Staehelin, *Actions of the rifamycins.* Bacteriological reviews, 1971. **35**(3): p. 290-309.

89. Floss, H.G. and T.W. Yu, *Rifamycin-mode of action, resistance, and biosynthesis.* Chemical reviews, 2005. **105**(2): p. 621-32.

90. Wehrli, W., *Ansamycins. Chemistry, biosynthesis and biological activity.* Topics in current chemistry, 1977. **72**: p. 21-49.

91. *Rifampin.* Tuberculosis, 2008. **88**(2): p. 151-4.

92. Vernon, A., *Treatment of latent tuberculosis infection.* Seminars in respiratory and critical care medicine, 2013. **34**(1): p. 67-86.

93. Telenti, A., et al., *Detection of rifampicin-resistance mutations in Mycobacterium tuberculosis.* Lancet, 1993. **341**(8846): p. 647-50.

94. Riley, L.W., *Drug-resistant tuberculosis.* Clinical infectious diseases : an official publication of the Infectious Diseases Society of America, 1993. **17 Suppl 2**: p. S442-6.

95. Feklistov, A., et al., *Rifamycins do not function by allosteric modulation of binding of Mg2+ to the RNA polymerase active center.* Proc Natl Acad Sci U S A, 2008. **105**(39): p. 14820-5.

96. Ramaswamy, S. and J.M. Musser, *Molecular genetic basis of antimicrobial agent resistance in Mycobacterium tuberculosis: 1998 update.* Tubercle and lung disease : the official journal of the International Union against Tuberculosis and Lung Disease, 1998. **79**(1): p. 3-29.

97. Huitric, E., et al., *Resistance levels and rpoB gene mutations among in vitro-selected rifampin-resistant Mycobacterium tuberculosis mutants.* Antimicrob Agents Chemother, 2006. **50**(8): p. 2860-2.

98. Mitchison, D.A., *Role of individual drugs in the chemotherapy of tuberculosis.* The international journal of tuberculosis and lung disease : the official journal of the International Union against Tuberculosis and Lung Disease, 2000. **4**(9): p. 796-806.

99. Chan, E.D. and M.D. Iseman, *Multidrug-resistant and extensively drug-resistant tuberculosis: a review.* Current opinion in infectious diseases, 2008. **21**(6): p. 587-95.

100. Bifani, P., et al., *The evolution of drug resistance in Mycobacterium tuberculosis: from a mono-rifampin-resistant cluster into increasingly multidrug-resistant variants in an HIV-seropositive population.* The Journal of infectious diseases, 2008. **198**(1): p. 90-4.

101. Jassal, M. and W.R. Bishai, *Extensively drug-resistant tuberculosis.* The Lancet infectious diseases, 2009. **9**(1): p. 19-30.

102. Niemi, M., et al., *Pharmacokinetic interactions with rifampicin : clinical relevance.* Clinical pharmacokinetics, 2003. **42**(9): p. 819-50.

103. L'Homme R, F., et al., *Clinical experience with the combined use of lopinavir/ritonavir and rifampicin.* AIDS, 2009. **23**(7): p. 863-5.

104. Irschik, H., et al., *The myxopyronins, new inhibitors of bacterial RNA synthesis from Myxococcus fulvus (Myxobacterales).* The Journal of antibiotics, 1983. **36**(12): p. 1651-8.

105. Srivastava, A., et al., *New target for inhibition of bacterial RNA polymerase: 'switch region'.* Curr Opin Microbiol, 2011. **14**(5): p. 532-43.

106. Artsimovitch, I., et al., *A new class of bacterial RNA polymerase inhibitor affects nucleotide addition.* Science, 2003. **302**(5645): p. 650-4.

107. Darst, S.A., *New inhibitors targeting bacterial RNA polymerase.* Trends in biochemical sciences, 2004. **29**(4): p. 159-60.

108. Cole, S.T., et al., *Deciphering the biology of Mycobacterium tuberculosis from the complete genome sequence.* Nature, 1998. **393**(6685): p. 537-44.

109. Cosma, C.L., D.R. Sherman, and L. Ramakrishnan, *The secret lives of the pathogenic mycobacteria.* Annual review of microbiology, 2003. **57**: p. 641-76.

110. Rodrigue, S., et al., *The sigma factors of Mycobacterium tuberculosis.* FEMS microbiology reviews, 2006. **30**(6): p. 926-41.

111. Zhang, Y. and W.W. Yew, *Mechanisms of drug resistance in Mycobacterium tuberculosis.* The international journal of tuberculosis and lung disease : the official journal of the International Union against Tuberculosis and Lung Disease, 2009. **13**(11): p. 1320-30.

112. Hu, Y. and A. Coates, *Nonmultiplying bacteria are profoundly tolerant to antibiotics.* Handbook of experimental pharmacology, 2012(211): p. 99-119.

113. Sambandamurthy, V.K., et al., *A pantothenate auxotroph of Mycobacterium tuberculosis is highly attenuated and protects mice against tuberculosis.* Nature medicine, 2002. **8**(10): p. 1171-4.

114. Sambandamurthy, V.K., et al., *Mycobacterium tuberculosis DeltaRD1 DeltapanCD: a safe and limited replicating mutant strain that protects immunocompetent and immunocompromised mice against experimental tuberculosis.* Vaccine, 2006. **24**(37-39): p. 6309-20.

115. Behr, M.A., *Evolution of Mycobacterium tuberculosis.* Advances in experimental medicine and biology, 2013. **783**: p. 81-91.

116. *<WHO World Health Organization report 2012>.*

117. Gideon, H.P. and J.L. Flynn, *Latent tuberculosis: what the host "sees"?* Immunologic research, 2011. **50**(2-3): p. 202-12.

118. Zhang, Y., et al., *Mode of action of pyrazinamide: disruption of Mycobacterium tuberculosis membrane transport and energetics by pyrazinoic acid.* The Journal of antimicrobial chemotherapy, 2003. **52**(5): p. 790-5.

119. Zhang, Y. and D. Mitchison, *The curious characteristics of pyrazinamide: a review.* The international journal of tuberculosis and lung disease : the official journal of the International Union against Tuberculosis and Lung Disease, 2003. **7**(1): p. 6-21.

120. Barry, C.E., 3rd, et al., *The spectrum of latent tuberculosis: rethinking the biology and intervention strategies.* Nat Rev Microbiol, 2009. **7**(12): p. 845-55.

121. Lilja, J.J., M. Niemi, and P.J. Neuvonen, *Rifampicin reduces plasma concentrations of celiprolol.* European journal of clinical pharmacology, 2004. **59**(11): p. 819-24.

122. Waksman, S.A., *Streptomycin and neomycin: an antibiotic approach to tuberculosis.* British medical journal, 1950. **2**(4679): p. 595-600.

123. *MMWR Weekly report January 7, 2005 Vol 53 and No. 51 (Center for.disease control and prevention.)*

124. Koul, A., et al., *The challenge of new drug discovery for tuberculosis.* Nature, 2011. **469**(7331): p. 483-90.

125. LoBue, P., *Extensively drug-resistant tuberculosis.* Current opinion in infectious diseases, 2009. **22**(2): p. 167-73.

126. Madariaga, M.G., U.G. Lalloo, and S. Swindells, *Extensively drug-resistant tuberculosis.* The American journal of medicine, 2008. **121**(10): p. 835-44.

127. Niyomrattanakit, P., et al., *A fluorescence-based alkaline phosphatase-coupled polymerase assay for identification of inhibitors of dengue virus RNA-dependent RNA polymerase.* Journal of biomolecular screening, 2011. **16**(2): p. 201-10.

128. Sarkar, S., W.T. Ma, and G.H. Sandri, *On fluctuation analysis: a new, simple and efficient method for computing the expected number of mutants.* Genetica, 1992. **85**(2): p. 173-9.

129. Hall, B.M., et al., *Fluctuation analysis CalculatOR: a web tool for the determination of mutation rate using Luria-Delbruck fluctuation analysis.* Bioinformatics, 2009. **25**(12): p. 1564-5.

130. Stewart, F.M., D.M. Gordon, and B.R. Levin, *Fluctuation analysis: the probability distribution of the number of mutants under different conditions.* Genetics, 1990. **124**(1): p. 175-85.

131. Jones, M.E., J. Wheldrake, and A. Rogers, *Luria-Delbruck fluctuation analysis: estimating the Poisson parameter in a compound Poisson distribution.* Computers in biology and medicine, 1993. **23**(6): p. 525-34.

132. Darst, L., *Find/Methods.* Antioch Review, 2010. **68**(2): p. 283-283.

133. Rosche, W.A. and P.L. Foster, *Determining mutation rates in bacterial populations.* Methods, 2000. **20**(1): p. 4-17.

134. Mitchison, D.A., *Prevention of drug resistance by combined drug treatment of tuberculosis.* Handbook of experimental pharmacology, 2012(211): p. 87-98.

135. Gillespie, S.H., *Evolution of Drug Resistance in Mycobacterium tuberculosis: Clinical and Molecular Perspective.* Antimicrob Agents Chemother, 2002. **46**(2): p. 267-274.

List of primers

Name	Sequence
B1	5’-ATG GTG TTG GCA GAT TCC CGC CA-3’
B2	5’-TTC ATC AAC AAC AAC ACC GGT G-3’
B3	5’-GAG GCG CTG TTG GAC ATC TAC CG-3’
B4	5’-ACC ACC CAG GAC GTG GAG GCG AT-3’
B5	5’-GCC ACG TGG TGG CAC AGG CCA ATT-3’
B6	5’-GGA TGC GCA AGT TTG CCC GGT CCA-3’
B7	5’-CAA GGT CAC CCC GAA GGG TGA GA-3’
B8	5’-TTG GTG TGC CCA CAG CGG CTG GA-3’
B9	5’-GAT GGA GTG CTG GGC CAT GCA GG-3’
C1	5’-GTG CTC GAC GTC AAC TTC TTC GA-3’
C2	5’-CGT GAT CAC CTC GGT CGA CGA GG-3’
C3	5’-GAA CTT CGA CAT CGA CGC CGA AG-3’
C4	5’-CAA GTC GCT TTC CGA TCT GCT CA-3’
C5	5’-CAA TGC CGA CTT CGA CGG TGA CC-3’
C6	5’-ACC ACG CTG GGC CGG GTG ATG TT-3’
C7	5’-GAT CAT CAC CAT CGT CGA CTC CG-3’
C8	5’-GAG GCC GGC AAC GTC ATC GTC GAG-3’
C9	5’-CAT CGT TCC TGA CGA CGG CGG TGA-3’
C10	5’-GTG AGC CCG CGG CCG GCC GTC CGG-3’
SB1	5’-GTG CTG GAA GGA TGC ATC TT-3’
SB2	5’-CAG ATC GTG GAG CGC TTC-3’
SB3	5’-AGA ACC AGA TCC GCG TG-3’
SB4	5’-AAC CCG TTC GGC TTC AT-3’
SB5	5’-TGG GTA CCG GTA TGG AAC T-3’
SB6	5’-TGC TCA CCT CGA TCC ACA T-3’
SB7	5’-GAG CTG GTC CGC GTC TA-3’
SB8	5’-GGT CTG CTC GGC TCG AC-3’
SB9	5’-CGC TTC GGT GAG ATG GAA-3’
SC1	5’-GTG CTA GAC GTC AAC TTC TTC GA-3’
SC2	5’-GCC CCG AAG GAT CTG GAA AA -3’
SC3	5’-ATC AAG AAG CTC ATC GAG AAC-3’
SC4	5’-ATC TGC TCA AGG GCA AGC A-3’
SC5	5’-AGA TGG CCG TGC ACC TT-3’
SC6	5’-CGT TCG TCA ACG AGC AGA T-3’
SC7	5’-GGT CTG GTG ACC AAC CCG AGG-3’
SC8	5’-GTC CGC TCG GTG CTG ACC TGC-3’
SC9	5’-TGG CTG TCG GCG GCG TCG TTC-3’
SC10	5’-CTC TCG AAG CGT CAG CGT CTG-3’